PARTICLE LABELING FOR SEDIMENT SOURCE TRACKING ON HILLSLOPES

BY

PAUL R SCHUMACHER

THESIS

Submitted in partial fulfillment of the requirements
for the degree of Master of Science in Agricultural and Biological Engineering
in the Graduate College of the
University of Illinois at Urbana-Champaign, 2015

Urbana, Illinois

Adviser:

Professor Prasanta K. Kalita

Abstract

Soil erosion on hillslopes is a dynamic process, which evolves temporally and spatially. Sediment source tracking can be used to identify the areas within a watershed where erosion is greatest. This study evaluated three sediment source tracking techniques, rare earth element (REE) particle labeling, interrupted rills, and ground based LIDAR, on slope surfaces under simulated rainfall. Laboratory rainfall simulations were conducted sequentially on 24 hr intervals to measure the cumulative effects of rainfall erosivity. Two bare soil plots, plot 1 and plot 2, measuring 3.6 m in length and 0.75 m in width were divided into three equal source sections along the length of the plot.

Various REE tracers were applied to different plot sections. As a result of high tracer enrichment in plot runoff, the REE technique overestimated plot sediment yield. However, trends in runoff tracer concentrations suggested that the top plot sections contributed most to sediment yield. The interrupted rill method was conducted in three phases, each with a different plot length, and relied on the assumption that each phase followed the same sedimentation process. The top section of plot 1 and the middle section of plot 2 were found to have the highest sediment displacements. The ground based LIDAR method also overestimated plot sediment yield. 3-D surfaces attained through this method suggested the bottom section of plot 1 and the top section of plot 2 had the highest sediment displacements. Data supports the theory that LIDAR performance increases with greater soil displacement. Further studies involving tracer enrichment, interrupted rill sedimentation processes, and LIDAR precision could increase these techniques' effectiveness at predicting eroded sediment sources.

Acknowledgments

I would like to express my deep appreciation for the efforts of the following people who helped bring this project together.

Dr. Prasanta Kalita, for his guidance and support not only throughout my project, but my entire academic career at the University of Illinois.

Dr. Rabin Bhattarai, for his patience and insight whenever I needed help

Dr. Richard Cooke, Dr. Paul Davidson, and Dr. Maria Chu, for their enthusiasm in the soil and water engineering discipline.

Mr. Rudiger Laufhutte, for his laboratory expertise with ICPMS analysis

The Academic Staff, for all the hard work they do to keep things going

The Soil and Water Cohort, for insight and constructive criticism

Table of Contents

List of Tables

List of Figures

Chapter 1

Introduction

Eroded sediments are usually considered the main source of pollution in rivers and streams (EPA, US Environmental Protection Agency, 1998). According to the Environmental Protection Agency (EPA), sedimentation has impaired 84,503 rivers and stream miles (12% of the assessed and 31% of the impaired river and stream miles) in the United States (EPA, US Environmental Protection Agency, 2000). Some of the most significant sources of sediment pollution are agriculture, construction, urban runoff, and mining. It must also be taken into consideration that many contaminants, e.g., phosphorus and heavy metals, attach themselves to sediment particles. Once attached, sediment erosion provides a convenient mode of transportation for attached contaminants. (Sediment runoff rates from construction sites are often 10 to 20 times greater than agricultural lands (United States Environmental Protection Agency, 2000).) Heavy sediment loading and the presence of other contaminants in construction site runoff can have major impacts on the physical, chemical, and biological processes of waterways. Some of the greatest sediment runoff rates originate from hillslopes. As a result, land managers have begun to employ best management practices (BMPs) on hillslopes to try to control erosion.

Information tracing eroded sediment back to its source would guide the implementation and development of BMPs. However, most traditional erosion studies are limited to spatially and temporally averaged data. Spatially distributed data is needed to better understand soil erosion dynamics on hillslopes and to evaluate the on and off site impacts of erosion. In an effort to

improve the availability of this spatially distributed data, sediment source tracking theory has been developed over the recent decades.

Surveying methods of sediment source tracking, which take physical measurements of soil surfaces, have been widely used (Vinci et al., 2015). These methods have also been rapidly developing with the advances in remote sensing technologies such as LIDAR and photogrammetry (Vinci et al., 2015). Traditional runoff sampling methods have been employed, but in these methods it is difficult to obtain source representative samples without altering the landscape or other special provisions. As a result particle labeling technology has emerged to track sediment mass movement for soil erosion. Particle labeling is a method that involves tagging soil particles with a known concentration of tracer material. Inferences about eroded sediment sources can then be made based on tracer concentrations in the eroded sediments.

Despite the continued effort to apply these methods to sediment source tracking theory, there has been little consensus amongst researchers on proper methodologies. Also, little research have been done validating these methods against one another. The motivation for this study was to evaluate several sediment source tracking techniques simultaneously under simulated rainfall conditions. The results would determine method performance and help to identify key challenges in sediment source tracking theory.

Chapter 2

Objectives

The main objective of this research was to investigate sediment movement on hillslopes under simulated rainfall conditions. The specific study objectives were:

1. Develop a consistent and repeatable environment to analyze sediment source tracking techniques under simulated rainfall.

2. Investigate and develop rare earth element particle labeling methods for sediment source tracking on hillslopes under simulated rainfall.

3. Investigate and develop additional techniques for sediment source tracking on hillslopes under simulated rainfall.

4. Evaluate sediment source tracking methods effectiveness at predicting sediment source locations on hillslopes.

Chapter 3

Review of Literature

Sediment source tracking procedures are often tedious in nature. As a result, many sediment source tracking methods and procedures have been developed over the years. To gain a better understanding of some of the key issues and motives behind sediment source tracking theory, a brief review of literature was prepared.

3.1 Best Management Practices

Established vegetation naturally dissipates energy from rainsplash and runoff protecting bare earth from erosion. However, anthropogenic activity often disturbs natural vegetation, leaving the soil bare and exposed to an onslaught of erosive properties. A single storm event over bare earth could massively degrade a landscape and create heavily sediment laden runoff. If not managed properly, this runoff could make its way into streams, river, or lakes. Best management practices (BMPs) are practices, or combinations of practices, that have been determined to be most effective and practical at mitigating pollution generated from diffuse sources. Land managers and engineers strategically implement BMPs to stabilize areas with high erosion potential. BMPs for erosion mitigation are generally divided into two categories, temporary site stabilization and permanent site stabilization.

Construction activates often disturb natural vegetation leaving work sites vulnerable to erosion. Temporary site stabilization methods are designed to mitigate erosion or control sediments until natural vegetation can be reestablished. BMPs for erosion control are designed to reduce the amount of erosion that happens on a site. Adding cover to bare soil surfaces mimics the effect natural vegetation. Soil can be covered with natural materials such as mulch

and compost or manmade materials like rolled erosion control products. A common form of rolled erosion control products implemented at construction sites are erosion control blankets (ECBs) which are stapled or staked over bare soil. ECBs are degradable products commonly made out of excelsior fibers, straw, or coconut fibers which are woven, glued, or stitched into mesh or thread. Slope length is also a factor that can be controlled to reduce erosion. Slopes checks are commonly added to hillslopes and channels to reduce slope lengths, thereby reducing runoff energy.

BMPs for sediment control are also used for temporary site stabilization. Sediments are susceptible to being transported off site once they have been detached from the soil mass. Sediment control methods are designed to keep sediments on site and out of river, lakes, and streams. Sediment can be controlled by reducing the speed of runoff that exits the site. This slowing reduces flowing water's sediment transport capacity, allowing sediments to settle. As a result many sediment control devices are placed in areas of concentrated flow and are designed to temporary retain runoff causing ponding. Some common sediment control methods are ditch checks, sediment basins, inlet protection, and perimeter control. Temporary methods are only designed to stabilize areas until natural vegetation is reestablished to protect the soil. However, in some instances natural vegetation may not be sufficient to control erosion requiring, more permanent measures.

Permanent site stabilization is often required in areas of concentrated flow, e.g., ditches and streams, and areas with steep grade changes. Erosion will occur when the shear stress created by stream power is greater than the critical shear stress of the channel bottom. Grade control structures and check dams are permanent BMPs introduced to reduce stream power. Turf reinforcement mats can also be used to permanently increase critical shear stress of channel

bottoms. Permanent site stabilization methods are also necessary when land management practices prevent natural vegetation from returning, e.g., agriculture. Conventional agriculture can leave cropland bare for months out of the year, making it highly susceptible to erosion. BMPs such as cover cropping and reduced tillage are popular methods to protect bare soil. Grassed waterways are an effective BMP to control concentrated flow over bare soil which may cause the formation of deep rills or gullies. Also, cropland with higher gradients may benefit from terracing to reduce slopes lengths.

One parameter that all BMPs for erosion and sediment control have in common is maintenance. Proper maintenance is essential to assure that BMPs perform effectively for the duration of their design life. Maintenance cost should be taken into consideration in BMP design. BMP design and implementation is a site specific process. A designer must identify areas susceptible to erosion and choose appropriate BMPs. Studies identifying areas of high erosion potential will increase an engineer's ability to strategically implement BMPs. An important step in understanding this issue is first recognizing the erosive processes of water on hillslopes.

3.2 Water Erosion Mechanics on Hillslopes

Soil erosion involves the breakdown, transport, and redistribution of soil particles by forces of water, wind, or gravity (NRCS, 2007). Soil erosion can be defined in relation to specific erosion processes and erosive forces. The process of erosion by water starts with the detachment and transport of soil particles by impact force of raindrops and drag force of overland flow. The dominance of one force, or a vector combination of the two controls the processes of sediment detachment and transport. In order for sediments to be transported, they must first be detached from the soil mass or in a detached state.

The erosion process can be either detachment limited or transport limited. This limitation is determined by the maximum amount of sediment a flow can carry, the sediment transport capacity. The erosion process is detachment limited when the sediment load in the flow is below the sediment transport capacity. In this case the flow carries all the detached particles outside the spatial unit. When the sediment concentration in the flow is above the sediment transport capacity erosion becomes transport limited. The flow does not have enough energy to transport all the detached particles outside the spatial unit. If erosion is transport limited, deposition is likely to occur. Deposition occurs when a particle settles out of the flow after being detached and transported to a new located within the spatial unit. From a geomorphological prospective based on hillslope evolution, erosion processes can be grouped into two distinct groups, interrill and rill processes.

In interrill processes entrainment is primarily caused by rainsplash energy. Interrill processes include splash, sheetwash, rainflow erosion. Splash erosion is caused by the kinetic energy of raindrops. Raindrop energy causes sediment to detach from the soil mass and to splash upon impact. A measure of the energy of an impacting droplet is raindrop erosivity, which can change with raindrop size and velocity. The ease of which the soil mass yields to raindrop impact is called the detachability of the soil. The remaining two forms of interrill erosion, sheetwash and rainflow, require overland flow. Overland flow exists where rainfall rate exceeds surface infiltration capacity (HORTON, 1945). This thin sheet of flowing water has little energy to scour the soil surface. Therefore, the majority of particles transported by overland flow have been previously disturbed by raindrop impacts.

The disturbed particles quickly separate into sediment load and bed load. Sediment load particles are small enough to be transported by the shallow sheetwash alone. The transport of the

sediment load is referred to as sheetwash erosion. The bed load particles are lager particles that cannot be transported by shallow overland flow alone. These particles will remain on the soil surface until entrained by the force of raindrops impacting shallow overland flow. This process of raindrop induced transportation is referred to as rainflow erosion (Moss, 1988). Overland flow is often considered to be uniform in depth across the hillslope. The onset of rill erosion begins when overland flow becomes concentrated in numerous small channels and depressions.

The transition from interrill to rill erosion processes is critical for the geomorphic evolution of a hillslope. Rill erosion is primarily caused by runoff energy. Rills form in localized depressions on the hillslope where overland flow accumulates as it traverses downslope. If the transport capacity is higher than the sediment load provided by the incoming overland flow, the accumulated flow will scour the bed for more sediment. This scouring creates channels and contributes to the evolution of rill networks. A rill network will begin near the bottom of a slope and will gradually evolve up the slope as smaller rills begin to feed into lager rills (HORTON, 1945).

Erosion mechanisms on hillslopes are extremely complex. Erosion processes may occur in isolation, simultaneously, or sequentially. As a result it is important to study the effects of both rainfall and runoff energy on a hillslope. Hydrogeomorphological studies operating under natural precipitation regimes often cannot provide consistently repeatable conditions. Consistent hydrological events are necessary for the development, calibration, and validation of various erosion models. A constant controlled rain can be achieved with a well-functioning rainfall simulator. This makes rainfall simulation an ideal tool for studies involving erosion, infiltration, and other geomorphological areas requiring the replication of natural rainfall characteristics (Aksoy et al., 2012). A rainfall simulator grants the user the flexibility to take many

measurements without having to wait for natural rain. Also, rainfall simulators allow for the adjustment of rainfall intensity and duration which is otherwise uncontrolled in natural systems. These advantages over natural rainfall conditions have led to the development of many different rainfall simulator designs.

3.3 Rainfall Simulation Overview

The design of a rainfall simulator depends mostly on its intended purpose. Rickson et al., (2006) used a rainfall simulator consisting of only one nozzle to quantify rain splash erosion in splash cups with a diameter of only 7.7 cm (Rickson, 2006). On the other hand Moore et al., (1983) describes the highly complex Kentucky Rainfall Simulator, which was designed to be effective up to a plot size of 4.5m by 22m (Moore et al., 1983). Smaller simulators are often inexpensive, easy to setup, and simple to use. On the contrary, larger simulators are often expensive, complex, and labor intensive. This makes the mobility of larger simulator generally impractical. Regardless of the rainfall simulators size it must meet the following criteria to be effective in a research sense. First the simulator must be easily controllable and remain constant for the duration of the experiment. Next, the drop size distribution and velocity should be similar to natural rainfall. Finally, the spatial distribution should be even and random (Clarke and Walsh, 2007).

There are two common types of rainfall simulator, non-pressurized and pressurized. Many non-pressurized systems generate rainfall when water drops form around an orifice connected to a water supply. The water droplet size can be adjusted by increasing or decreasing the diameter of the orifice. These types of simulators are often referred to as drip type simulators. These systems are ideal for smaller plot sizes and are typically simple to set up and operate. When designing a simulator for field trials in the rainforest Clarke & Walse et al.,

(2007) chose this design because of its simplicity, portability, and hardiness. Using drip simulators for large plots becomes cumbersome because the area of coverage per drip orifice is low and the number of drip orifices required is proportional to the area of coverage. A practical way to upscale a rainfall simulator is to increase the area of coverage per orifice.

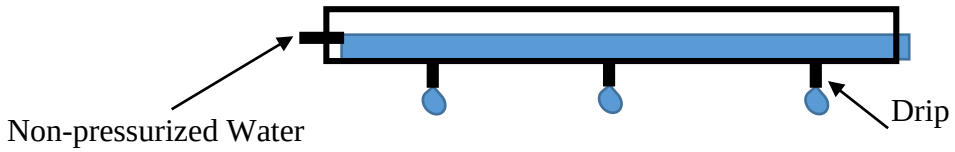

Figure 3.1 Basic non-pressurized rainfall simulator

Increasing the area of coverage can be achieved by pressurizing the water supply and adding a spray nozzle to the orifice. This type of rainfall simulator is referred to as a sprinkler type rainfall simulator (Figure 3.2). Its basic components include a pressurized water supply, one or multiple spray nozzles, and a structure to support the nozzle (Cerdà et al., 1997).

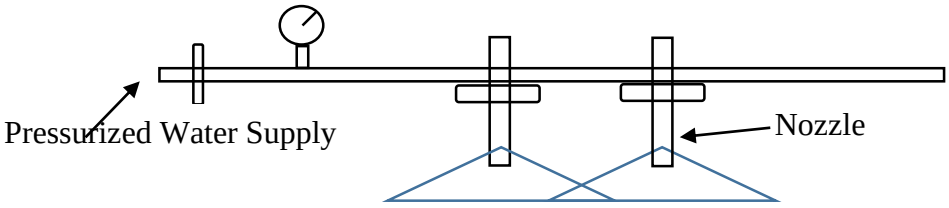

Figure 3.2: Basic pressurized rainfall simulator

Pressurized rainfall simulator come in many different configurations. The simpler systems have their nozzles fixed in one position. While other more complex systems may have

nozzles attached to rotating or oscillating booms. The Kentucky Rainfall Simulator is an oscillating type rainfall simulator. In this design a nozzle oscillates back and forth over an overspray pan with a gap in the middle (Figure 3.3). Every time the nozzle rotates over the pan water falls thru the gap. When the nozzle is not positioned over the gap the water is sprayed into an overspray pan and is returned to the pumping system. The dwell time, the time the nozzle is directed over the gap, is proportional to the rainfall simulation intensity. Increasing the oscillation frequency increases dwell time and therefore increases rainfall intensity (Moore et al., 1983). The purpose of this movement is to increase the quality of rainfall characteristics.

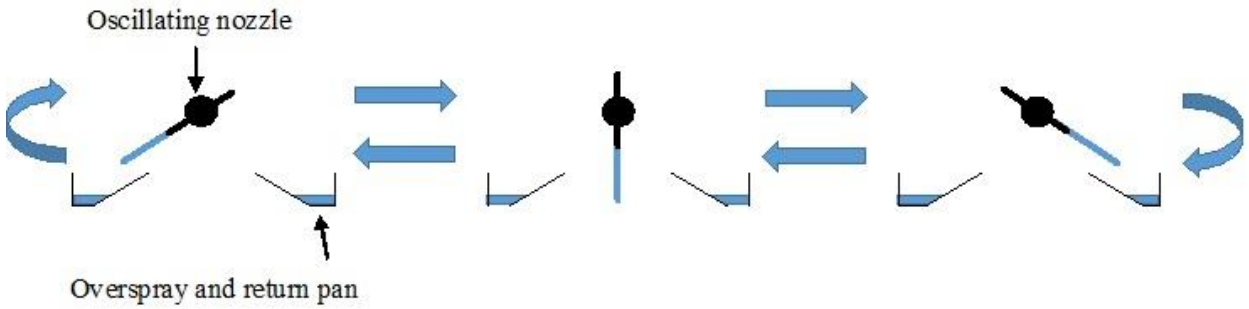

Figure 3.3: Oscillating rainfall simulator

3.4 Rainfall characteristics

High quality rainfall simulation is distinguished by the quality of rainfall characteristics. Some desirable characteristics for rainfall simulation used in erosion studies include spatial uniformity, rainfall intensity, droplet size, and droplet velocity. A common and useful measure of spatial uniformity is the uniformity coefficient, UC. UC is given by

$$UC = 1 - \frac{(\sum_{i=1}^{n} |y_i - d|)}{d * n}$$

where $y_i = measured\ depth\ of\ water\ caught\ or\ infiltrated,$

$d = average\ depth\ of\ water\ caught\ or\ infiltrated,$

$n = number\ of\ sample\ collected.$

When each measured value represents an equal area the UC indicates the degree to which the rainfall have been applied uniformly over the plot. Values of 0.8 or higher are acceptable for most applications (Huffman et al., 2011). Rainfall intensity is simply a measure of rain depth per unit time. This characteristic is especially important when calibrating a rainfall simulator. The raindrop size distribution should be similar to the distribution of the natural rainfall conditions being simulated. A flour pellet method supported by an image processing technique can be used to measure raindrop size distribution (Aksoy et al., 2012). When generating a raindrop size distribution one should expect that lower flow velocities result in larger droplets (Cerdà et al., 1997). For this reason, non-pressurized systems typically produce larger droplets than pressurized systems. The velocity of natural rainfall is accelerated by gravity to the droplets terminal velocity. In order to achieve terminal velocity, the rainfall simulator should be placed sufficiently high above the test plots for raindrop acceleration. The rainfall simulator itself may not be the only factor effecting rainfall characteristics.

The environment in which the simulator is subjected to is also going to greatly affects performance. One of the biggest issues with rainfall simulation is achieving an acceptable UC. When a rainfall simulator is placed outside, windy conditions can greatly reduce the simulators UC (Moazed, H Bavi, A Boroomand Nasab, S Naseri,A Albaji, M., 2010). Windy conditions may cause water droplets to drift outside or to one side of the test area, reducing the UC. Wind

barriers or screens are often employed in conjunction with outdoor rainfall simulators to combat this problem (Cerdà et al., 1997; Moore et al., 1983). Temperature and humidity may also affect rainfall characteristics. The variability of natural weather conditions has led to the construction of indoor rainfall simulators. Rainfall simulators located in a controlled indoor environment have less disruption from natural conditions (Clarke and Walsh, 2007). Well-functioning indoor simulators can provide consistently repeatable rainfall characteristics making them an ideal tool for erosion studies involving repetition.

3.5 Quantifying Erosion

In order to make scientific inferences about a subject, a measurement must be taken. Measurements, the means by which numbers enter science, may have qualitative or quantitative qualities (Narens, 2002). In regards to soil erosion, a useful measure of sediment yield can be expressed as volume of eroded material per unit area. Achieving this unit of measure has its own challenges. For these calculations, it is import to have a well-defined erosion area. This is usually not as pressing for experiments undergone in a laboratory setting because erosion plots can easily be constructed to dimensions specified by the experiment (Polyakov and Nearing, 2004; Lei et al., 2002). However, experiments which are undertaken on natural hillslopes may not have clearly defined boundaries (Deasy and Quinton, 2010; Brooks et al., 2014). In some outdoor studies it may be practical to mitigate this problem by installing barriers around the plot to create a well-defined area of interest (Vinci et al., 2015). Over the years there have been many methods developed to measure total eroded material. These methods can be grouped into two basic categories, surveying methods and sampling methods.

3.5.1 **Surveying Methods**

First, methods that survey the topography of the erosion area before and after an erosion event. Erosion can then be quantified by measuring the differences in spatial elevation. One of the more traditional methods of doing this is with erosion pins. Sirvant et al., (1997) installed fixed metal rods in natural erosion plots to be used elevation references. Every six months the soil profiles were measured in reference to the rod (Sirvent et al., 1997). A profilometer is another traditional instrument that is commonly used in the measurement of erosion, particularly rill erosion. To measure the topography of a rill, a profilometer is used measure the mean cross-sectional area of a rill. The length of the rill is then measured with a ruler. With this information rill volume can be determined.

Modern methods, particularly remote sensing methods, for terrain analysis are becoming increasingly popular. Remote sensing methods make it possible to acquire information without actually making physical contact with object. One form of remote sensing, Light Detection and Ranging (LIDAR), has proven to be a particularly useful tool for measuring soil erosion. LIDAR technology can produce digital elevation models (DEMs) of the soil surface. This technology measures location using a laser to illuminate and object and analyzing the reflected light. Object locations are then stored in a 3-D point cloud. DEMs can be interpolated from the measurements using a gridding method. An eroded sediment volume can be derived from surface DEMs produced before and after an erosion event. A LIDAR base unit can collect measurements from a stationary ground position or from a moving airplane. Ground-based LIDAR, often referred to as Terrestrial Laser Scanning, is preferred for most small scale erosion studies.

Ground-based LIDAR is used on smaller scales. This allows point to point measurement to be taken mere centimeters apart (Meijer et al., 2013). Arial LIDAR typically covers large areas at a time. Data storage constraints limit aerial point to point measurement capabilities. As a result DEMs produced from ground-based LIDAR measurements are much better representations of the true soil surface.

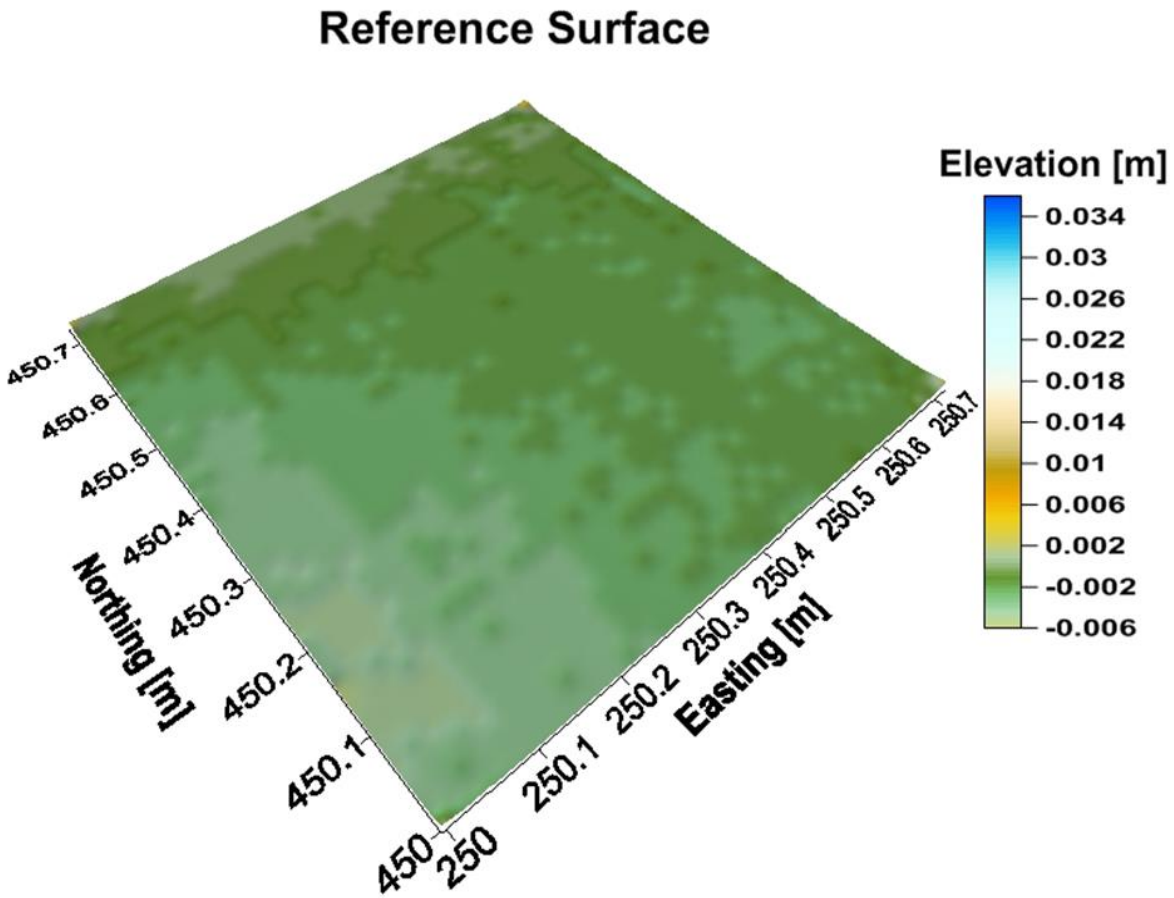

Figure 3.4: DEM created with point cloud from ground based LIDAR

Ground-based LIDAR can be an effective tool for erosion studies across a wide variety of temporal scales. (Vericat et al., 2014) demonstrated how repeat Terrestrial Laser Scanning can

be effective for measuring erosion at multiple temporal (event to annual) scales. Meijer et. al., (2013) used ground-based LIDAR to study erosion patterns in long-term tillage plots. Ground-based LIDAR has also proven scalability in the spatial aspect. This method has been used to monitor debris-flow in a large catchments (Blasone et al., 2014) and to track the advancement of eroding rills in a small plot scale study (Vinci et al., 2015).

Photogrammetry, another remote sensing technology using photographs to make measurements, has also been used to create DEMs for the analysis of soil erosion. This method employs various methods of optics and projective geometry to define points in 3D space. Photogrammetry is a delicate science which requires careful camera calibrations and orientations and extensive site preparation. (Gessesse et al., 2010) developed a method to utilize close range photogrammetry to measure rill development in a small field plot. The approach was adequately successful, but the method presented some challenges. A surface DEM is achieved by the aerial triangulation of many photographs taken from precisely positioned cameras. For practical reasons this method is constrained to small test plots. Issues also arose from camera distortion and the precision of ground control points effecting the precision of the DEMs.

Surveying method for measuring soil erosion also provide spatial information. With survey information it is easy to identify areas of erosion and deposition. This knowledge is useful for researchers and land managers in the development of best management practices. However, these methods are only capable of producing representations of the true surface through measurement. Measurement, physical or remote, is the main challenge associated with these methods. Some ground-based LIDAR units have a measurement tolerance of 2 to 6 mm (Peter Heng et al., 2010). Erosion and deposition causing surface elevations changes below tolerance may be difficult to quantify. The accuracy and precision of each method is dependent

on measurement techniques. Vinci et al., (2015) compared a ground-based LIDAR and profilometer method while studying rill formation on a hillslope and reported a difference of approximately 15%.

3.5.2 **Sampling Methods**

Physical collection and measurement is another method for measuring sediment yield. Runoff flowing past the plot outlet is the conduit for sediment transport. The determination of sediment concentration in water collected from the plot outlet will determine the total sediment yield from the plot. The method for the determination of sediment yield varies form study to study for practical reasons, e.g., runoff volume and sediment concentration. In most cases it is not practical to analyze the entire volume of collected runoff. In these instances a representative sample should be used to determine the sediment concentration in the runoff. The American Society for Testing and Materials recommends three methods for determining sediment concentration in water samples, evaporation, filtration, and wet-sieving filtration (ASTM, 2013). The evaporation method is recommended for sediments that settle within an allotted storage time. If the sediments fail to settle within the allotted storage time, the filtration method is recommended. The wet-sieving method is used when sand-size and clay-size particle concentrations are required.

The required sampling regime is to achieve total sediment yield is dependent on runoff volume and runoff storage capacity. In some cases, the experiment may be scaled so as the entirety of the runoff can be contained. Bhattarai et al., (2011) collected runoff from a small laboratory soil bed in 23 L glass carboys. Two representative samples were taken from each bottle for sediment analysis. In larger studies it may not be practical or even possible to collect all the runoff from the plot outlet and achieve a representative sample. (Deasy and Quinton,

2010) conducted a field scale experiment collecting surface runoff in a tank located near the outlet. A portion of the runoff was diverted to waste through a tipping bucket sample splitter. This technique requires the collection of only a fraction of the total runoff yet still provides a representative sample. If runoff discharge can be monitored, it is also possible to achieve an estimate of sediment movement by sampling on a fixed time scale thorough the duration of the flow. Concentrations in samples can be multiplied by water discharges to achieve sediment discharges (ASTM, 2013).

Sampling Methods are a robust and effective means of determining sediment yields from an erosion plot. As long as sampling regimes and plot borders are maintained these methods are effective for determining sediment yields in studies of various temporal and spatial scales. However, sediment yields only provide researchers with enough information to know that erosion is occurring. A critical piece of missing information is where the erosion is occurring within the plot. Without a spatial aspect, highly erodible areas cannot be targeted for mitigation. Surveying methods could be employed to achieve this information, but impose certain challenges. Surveys can be highly technical and often expensive. In addition vegetation and other forms of ground cover can render them useless. With these challenges in mind, researchers have developed techniques to identify areas of erosion and deposition with sampling methods. This area of science is known as sediment source tracking.

3.6 Particle Labeling for Sediment Source Tracking

3.6.1 Tracers

A method for sediment source tracking is sediment fingerprinting. Sediment fingerprinting is a process measuring in the inherent properties of sources materials. Eroded materials are then analyzed for these source unique properties (tracers). A tracer is a measurable

physical property of soil particles that can be used to differentiate it from other soil particles. Tracers can be naturally occurring or introduced manually. With this analysis estimations may trace where sediments came from and which areas contributed the most. There are several different types of tracer methods that can be used in erosion experiments.

One method of sediment fingerprinting is magnetism. Ventura et al., (2002) mixed plastic beads coated with a magnetic tracer into the soil. His experiments on interrill erodability were conducted in a lab. The plastic beads were 2.54 mm on average in diameter; this is very large in comparison to soil particle sizes. Despite this difference, Ventura measured that the tracer beads were transported at the same concentration that they were mixed with the soil. A magnetometer was used to identify areas of detachment and deposition (Ventura et al., 2002).

Radiometric methods are also used in sediment fingerprinting. Huisman et al., (2013) used a model to predict sediment load contributions of specific areas in a Wisconsin watershed. The model used fallout radionuclides already present in the soil to make these predictions. Soil core samples were taken at various locations within the watershed to characterize radiometric properties. The model was designed to study not only spatial aspects of sediment transport but, also temporal aspects. It was found that upland areas are the main contributors to in stream suspended sediment followed by stream banks (Huisman et al., 2013).

Another tracer method for sediment fingerprinting is introducing rare or absent elements to the sediment in the testing areas. The concentration of the introduced element in the eroded material can then be used to make estimations of the tagged area's contribution to the total sediment load. Olmez et al., (1994) applied a sediment fingerprinting technique to measure the impact of bioturbation on sediments as a function of time in the Massachusetts Bay. In this study sediment was removed from the bay and labeled with noble metals such as gold and silver. After

the sediment was tagged, it was reintroduced into the bay near a proposed waste water treatment plant outfall and tracked. Tracer quantifications were measured with an instrumental neutron activation analysis (INNA) method (Olmez and Pink, 1994).

Gold and silver are not the only element that can be added to the sediment. Lei et al., 2006 utilizes lanthanide series rare earth oxides (REO) as tracers to measure rill erosion properties. Lei studied the formation of rills in a flume under various flow and slope conditions. The rill was divided into several sections, each of which was tagged with a unique REO. By measuring the concentrations of the rare earth elements (REEs) in the runoff Lei was able to make estimations spatially of eroded amounts along the rill (Lei et al., 2006).

In an effort to make sediment fingerprinting more applicable for larger field scale experiments, Deasy et al., (2010) developed a tracer application method that did not require soil excavation, mixing, and redistribution. Deasy simply applied REOs such as galolinium, praeodymium, samarium, neodymium to the soils surface via a backpack sprayer. The REOs came in the form of powders and were mixed with distilled water before application to the soil surface. Deasy carried out his experiments on an agricultural hillslope in Loddington, UK.. He concluded that the majority of the sediment was coming from the upland areas (Deasy and Quinton, 2010).

3.6.2 Rare Earths Oxides

Recently REOs as tracer have come to the forefront of sediment tracer technology (Zhu et al., 2011; Lei et al., 2006; Deasy and Quinton, 2010). Rare earth elements are comprised of lanthanide metals, a group of 15 elements with atomic numbers ranging from 57 to 71. All lanthanides have similar chemical properties to lanthanum (La). Two additional elements, yttrium (Y) and scandium (Sc), which have similar physiochemistry to lanthanides are also

referred to as REEs. For this reason the terms lanthanide and REE are often used interchangeably. The lanthanide series corresponds to the filling of the seven 4f orbitals. Since the 4f orbitals are in the interior of the atom, additional electrons does not add to the atomic size. Due to an increasing nuclear charge, the radius of the elements actually decreases going from left to right, a phenomenon known as lanthanide contraction. The most common valence for lanthanides is (+3), although some can also be found in the (+2) or (+4)(Zumdahl and Zumdahl, 2014).

REEs are relatively abundant in the earth's crust (Liang et al., 2005). Some REEs are even more abundant than copper or lead. The term 'rare' does not refer to the REEs relative abundance in nature, but it implies that REEs are not present in pure ore deposits. The REEs must be extracted from the ore chemically. The desired REEs are leached out with various acidic or alkaline reagents. These intensely chemical procedures have made it difficult for REEs to be mined in the United States and other developed countries due to strict environmental sanctions. Nearly 95% of the world's REEs are supplied by China where environmental regulations are less stringent and in some cases non-existent (EPA, US Environmental Protection Agency, 2012).

The magnetic and spectroscopic properties of REEs make them suitable for use in advanced material science and industrial applications. These materials are commonly used in technologies such as mobile phones, magnets, lasers, and batteries (Table 1.1). (EPA, US Environmental Protection Agency, 2012) The demand for these critical materials will continue to grow with the demand for technology. In recent years China has been cutting REE exports in order to secure a supply for domestic manufacturing. This has caused the price of REEs raise and has led to some concerns over supply (Eggert, 2011; Peck et al., 2015). The unavailability

of these materials could slow the development of important emerging technologies. Concerns over supply has prompted an increased effort to recover REEs from secondary sources through recycling.

Lanthanides are widely considered to have relatively low toxicity to plants and animals (EPA, US Environmental Protection Agency, 2012; Wyttenbach et al., 1998). The chemical homogeneity of lanthanides is commonly used as a basis to predict similar toxicity across the entire series. Since the rare earth boom is a relatively recent phenomena, the effects of rare earth exposure is not completely understood. In general, excess exposures to one or many REEs may lead to a multitude of responses (Chen et al., 2014; Gonzalez et al., 2014). Effects of rare earth on humans has been given the most attention near rare earth mines where neighboring residential communities are at high risk for exposure (Liang et al., 2005; Gonzalez et al., 2014).

Lanthanide's maximum valance of 3 or 4 and their ionic radii which is similar to that of Ca^{3+} allow them to easily bond with sediment particles when mixed into soil aggregate. Once the tracers are mixed with the soil, these bonds prohibit the vertical movement of the tracers within the soil profile. Lanthanides are chemically stable and safe for the environment. Also, Lanthanides typically have very low natural background concentrations in soil making them ideal for tracer introduction studies.

Chapter 4

Materials and Methods

Based on the information provided in the literature review, the following methodologies were developed for sediment source tracking. All experimentation for this study took place at the University of Illinois between March 2014 and December 2014 in the Agricultural Engineering Sciences Building.

4.1 Laboratory Setup

A consistent laboratory environment eliminates some of the key challenges associated with repetitive erosion studies, e.g., weather conditions. In order to make inferences, it was imperative for experimental circumstances to be consistently similar. This required controlling erosion plot antecedent conditions and rainfall characteristics amid rainfall simulation. A consistent environment made it possible to make comparisons between various sediment source tracking techniques.

4.1.1 **Erosion Plot Overview**

An adjustable slope soil bed was used to define the erosion plot boundaries for these experiments (Figure 4.1). The bed's dimensions measure 3.6 m in length, 1.5 m in width, and 0.3 m in depth and was divided laterally to create two segregated compartments 0.75 m in width. The separate compartments allow for side by side comparison of plot treatments. The soil beds

walls were constructed out of heavy plate steel. It was mounted on a running gear to provide a sturdy base and to make it relatively portable. The slope adjustability was achieved by actuating two hydraulic cylinders located near the rear of the soil bed (Figure 4.2**)**. As the cylinders lift the rear of the bed, the fore bed pivots on bearings creating a positive slope to the rear. The slope of the bed was set to 15% for all experiments. A runoff collection tray is mounted to the front of the soil bed to collect sediment laden runoff from each bed compartment individually. Collected runoff was piped into 22 L glass carboys were it was stored for analysis. Holes were drilled in the bottoms of the bed compartments to allow for free soil drainage.

In order to assess sediment sources, each compartment of the soil bed was partitioned into three sections, up-slope, mid-slope, and down-slope. This created a total of six unique areas from which erosion was assessed. By dividing the soil compartments in this way, sediment source tracking experiments would estimate the fraction of contribution of each section to the total sediment load. This would determine valuable spatial information, such as the section where the most and least erosion occurred.

Figure 4.1: Twin soil beds positioned beneath rainfall simulator.

Figure 4.2: Hydraulic cylinders elevating soil bed to 15% slope.

4.1.2 **Soil Media**

The soil bed was loaded with top soil excavated from the Agricultural and Biological Engineering South Farms. The excavated soil was classified as a Drummer silty clay loam. When properly drained, this soil is a representative sample of prime farm ground, of hydrologic soil group B, and typically located on slopes of 0-2% (USDA, 2015). Laboratory testing of soil particle size by hydrometer method yielded sand, silt, and clay percentages of 15, 56, and 29 respectively. This particle size distribution is classified as a silty clay loam according to the soil texture triangle which is in agreement with the USDA Drummer soil series description. The soil was loaded identically into each compartment in two layers, the base layer and the surface layer.

The soil bed was not constructed specifically for these experiments. The soil bed was a fixture in the lab and had been used for many previous experiments and demonstrations. As a result, the soil bed was already filled to a depth of 25 cm with Drummer soil of the same type as described above. The existing soil layer was well compacted through wetting and drying cycles brought on by years of demonstrations and testing. Based on trials, the soil profile was not expected to erode more than 5 cm during the extent of the experiments. For quality, the top 15 cm of the profile was removed and replaced with virgin field soil. After excavation 10 cm of new soil was added in 5 cm lifts. The soil was leveled with a hand rack and compacted with a tamp to assure uniformity. The soil then underwent 3 wetting and drying cycles over the course of a week to encourage natural settling. The layer of old soil and new soil which together was approximately 20 cm in depth made up the base layer. This base layer of soil was intended to act as an impermeable layer and was not removed between experiments.

Much care was given to the preparation of the top 5 cm of the soil profile. This layer was the erodible layer for which erosion measurements were to be taken. Soil collected directly from the field had inconsistent soil moisture and was clotty. As a result, additional measures were taken to encourage aggregate soil uniformity in the top layer. Soil for this layer was air dried and passed through a 15 mm sieve. The drying and sieving process produced a consistent soil mixture with an average aggregate diameter conducive to mixing and packing. The methodology for top layer treatment and loading will be described in the following sections.

4.1.3 Rainfall Simulator Overview

In order to obtain consistent rainfall characteristics between trials, an indoor laboratory simulator was chosen for this experiment. The laboratory setting ensured similar antecedent conditions between trials by controlling the natural variables such as weather and wildlife. Achieving similar antecedent soil conditions between trials is essential in comparative erosion studies. The laboratory simulator was fixed and did not require time for setup or takedown. This reduces the time required for experimental setup making it easier to keep to a strict sampling regime.

The rainfall simulator utilized this study was a pressurized oscillating system. The oscillating rainfall simulator was located in southwest corner of the Agricultural Engineering Sciences Building's hydraulics lab at the University of Illinois. The system was fixed 10 meters above the soil bed to allow for simulated rainfall droplets to approach terminal velocity. The rainfall simulator consists of two parallel troughs, each with five elevated 0.09 m gaps equally spaced 1.1 m apart. A motor driven oscillating bar was mounted inside of the troughs. Veejet 80100 spray nozzles were fixed to the bar and connected to a tap water hose which supplied 41 kPa of water pressure. The nozzles oscillated over the trough gaps at a calibrated frequency to

simulate rainfall. Water that did not fall through the gaps landed in the trough and was recycled in the system. The motors that drove the oscillating bars were controlled by a computer program and could be adjusted to different frequencies, resulting in different rainfall intensities. The computer program required only two inputs, intensity and duration. This simulator was capable of simulating rainfall intensities up to 120 mm/hr. In Urbana, Illinois a 30 minute storm of this intensity has a return period of 100 years.

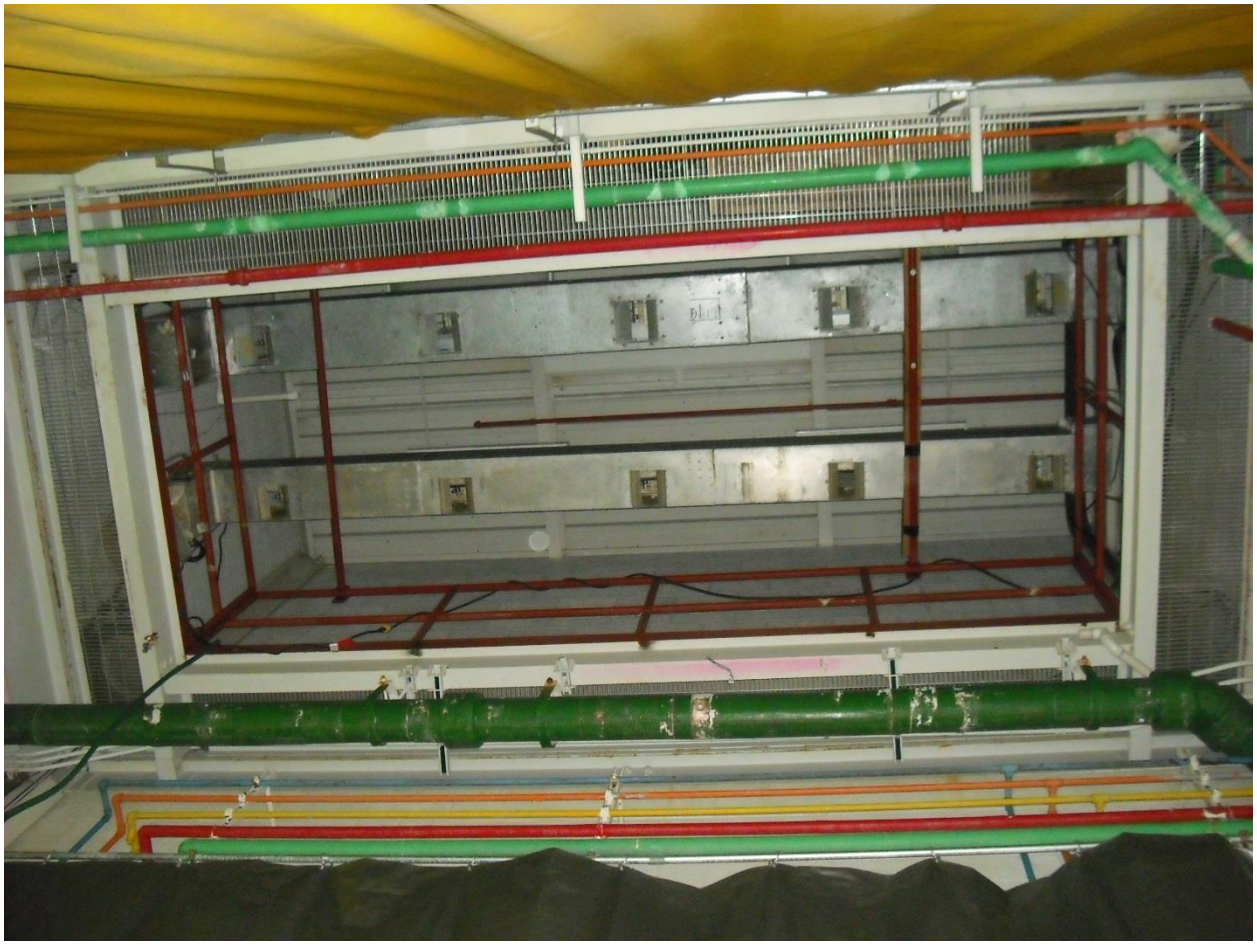

Figure 4.3: Hydraulics lab oscillating rainfall simulator.

This rainfall simulator was suspended above a steel grated floor with an underdrain, which prevented flooding of the lab when the simulator was in operation. The steel grates

covered the entire simulation area measuring 5.84 m by 2.8 m. Plastic coated curtains, which extended from the lab ceiling to the floor, could be draw around the simulation area to prevent excessive raindrop spattering and drifting. The soil beds were positioned directly under the simulator in the center of the simulation area to maximize rainfall uniformity. Uniformity over the test plots was measured by calculating the Uniformity Coefficient, UC.

UC was measured with an array of 33 rain gauges laid out over the soil plot (Figure 4.4**)**. In order assess the simulators UC, rain depth measurements were taken at each location after simulation. The target simulated storm intensity and duration for this experiment was 51 mm/hr for 30 minutes. The simulator intensity and duration chosen to assess plot rainfall UC was 51 mm/hr and 15 minutes. The rainfall simulator operates at a constant rate and after several trials it was determined that duration had little effect on the UC. As a result, duration was reduced from 30 minutes to 15 minutes for UC trails to conserve time and reduce water consumption.

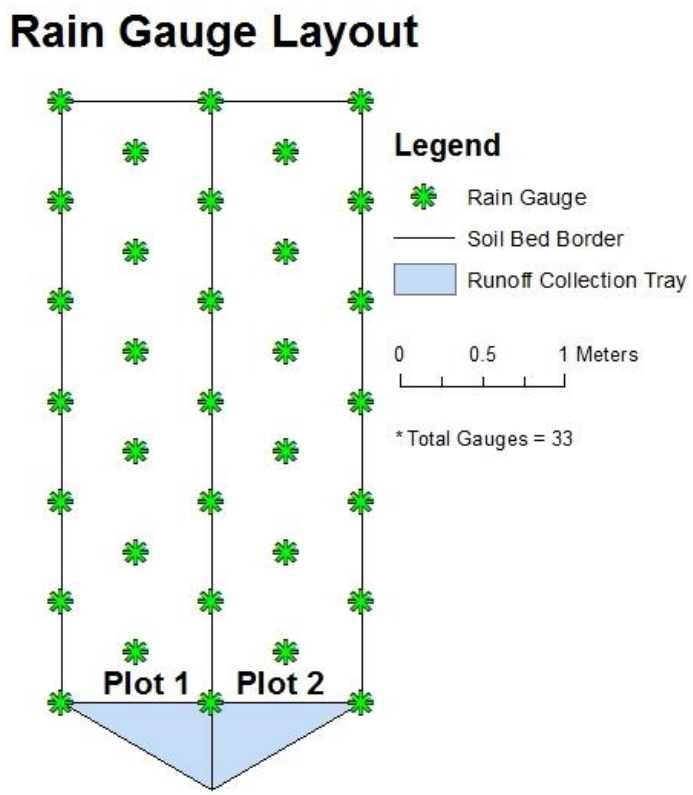

Figure 4.4: Plot rain gauge layout for measuring UC

4.1.4 **Runoff Sampling**

A well designed runoff sampling regime is critical to the success of rainfall/runoff water quality studies. Without a well thought out sampling program, samples can easily be skipped, mislabeled, or even contaminated. The target simulated storm intensity and duration for this experiment was 51 mm/hr for 30 minutes. The erosion plots utilized in these experiments contained the rainfall and runoff with three solid plot walls at the top and on both lateral sides of the plot. The runoff was directed down the slope to a perforated plot wall at the bottom of the slope which drained into steel collection trays (Figure 4.1). From these steel collection trays the runoff converged to a point and was funneled into a system of hoses. The hoses directed the

majority of the runoff into 23 liter glass carboys for temporary storage. A fraction of the runoff was collected into 600 ml glass sample bottles for analysis.

The runoff leaving the plot was diverted in two directions, the carboy and the sample bottle. This function was achieved with a manually operated duel shut off valve. (Figure 4.5) The first shut off was connected to a short length of hose which flowed directly to the carboy, while the second shut off was connected to short length of hose fused to a bottle lid. In this configuration the sample bottle could be attached directly to the system, minimizing the chances of spilling the sample and reduced the labor requirements for sampling. A sample could be taken simply by closing the valve leading to the carboy and opening the sampling valve. Samples were taken from both plots 1 and 2 at regular five minute intervals for the entire duration of the 30 minute experiment. An additional sample was taken at the beginning of each rainfall to represent the "first flush" runoff.

Temporal aspects of the sampling program where also recorded. The length of time after the simulation began until runoff started was recorded for each experiment. Flow rate was also calculated at the time each sample was taken. The flow rate was determined by recording the amount of time it took to fill each sample and by measuring the volume of each sample. Flow rate measurements could help to determine time of flow concentration. In addition inferences about infiltration rate could be drawn from temporal measurements.

Figure 4.5: Runoff sample collection apparatus

Runoff was collected in the glass carboy containers for the duration of each rain simulation. When the carboy filled, the shut off valve was closed and the apparatus was transferred to a new carboy to begin filling. After the 30-minute simulation, runoff continued to be collected until it ceased. The total runoff volume from each plot was measured by emptying the corresponding carboys into a 100 liter graduated bucket. After the volume was recorded, the contents of the bucket was stirred and three representative 600 ml samples were taken for sediment analysis. Special care was taken with bucket mixing to ensure sample uniformity. These samples where then appropriately labeled and send to the lab for analysis.

4.1.5 **Sample Analysis**

After each rainfall simulation all samples were processed in the lab for sediment concentration. The methodology used for determining the sediment concentration in the runoff sample was an adaptation of a standard adopted by ASTM, Designation: D3977 – 97 Standard Test Methods for Determining Sediment Concentrations in Water Samples. The Evaporation test method was deemed most applicable for sample analysis.

Three masses are required to calculate sediment concentration in parts per million, ppm. The first mass was that of the wet sample and the sample bottle. Once these measurements were recorded the samples were placed in a drying oven for 48 hours at 105˚C. The now dry samples were removed from the oven and allowed to equilibrate at room temperature. The mass of the sample bottles where then determined for a second time to measure the mass of the bottle combined with the dry sediment within. The sediment was then removed and the bottles where washed. A final measurement of the bottle mass was then taken. By subtracting the mass of the bottle from the previous two measurements, the mass of the wet sample and the mass of the dry sediment could be determined. The sediment concentration in ppm, C, was then calculated by dividing the mass of the dry sediment by the mass of the wet sample and multiplying the result by one million. A scale with a precision of one hundredth of a gram was used for all measurements.

Once the concentration in ppm was determined it was converted to mg/L, a more appropriate labeling for sediment analysis:

$$C_1 = \frac{C}{1.0 - C * 622 * 10^{-9}}$$

where C_1 is the concentration in mg/L, and the bulk density of the sediment is assumed to be 2.65 kg/cm^3 (ASTM 2013).

Figure 4.6: Runoff samples in the drying oven.

Select samples required additional analysis to determine REE concentration. These samples included runoff samples taken directly from the total runoff bucket and plot soil samples to determine REE concentrations in the plot soil. Three runoff samples were taken from each bucket during testing. After evaporation in the oven, sediment residue was combined to create a single representative sample. Plot soil samples were taken at randomly distributed points and dried in the oven. All sediment/soil samples were ground to a fine powder using a mortar and

pestle to ensure sample uniformity. The samples were sent out to the University of Illinois School of Chemical Science's Microanalysis Laboratory located in Noyes Laboratory of Chemistry for elemental analysis.

The REE analysis was carried out in the Microanalysis Laboratory through the use of Inductively Coupled Plasma Mass Spectrometry (ICPMS). ICPMS is a method of mass spectrometry which uses high temperature inductively coupled plasma to convert elements in a sample to ions which are then separated and detected with a mass spectrometer. The mass to charge ratio is used to determine an elements concentration in a sample. The machine was externally calibrated with standard solutions of each REE in question. The sediment samples were prepared for analysis by first digesting the sediments in nitric acid (HNO_3). The digested sample was then prepared to a 1:100 solute/diluent solution. The interaction between original sample REE concentration and HNO_3 digestion was measured with a blank sample. A HNO_3 correction factor was then applied to all REE sample analysis.

4.2 REE Particle Labeling Methods

Previous particle labeling experiments carried out by (Lei et al., 2006) and (Polyakov and Nearing, 2004) have shown that REE make viable tracers for sediment source tracking studies using a laboratory soil bed. (Deasy and Quinton, 2010) also utilized REE tracing methods in filed scale studies under natural weather conditions. However, when it comes to methodology there seems to be no basic consensus. This is especially true when it comes to introducing tracers to soils. Therefore studies to address each application methods capacity for sediment source tracking are needed. This study will compare two REE tracer application methods side by side.

4.2.1 **REE Application Methods**

Literature has cited several different tracers application methods which can be grouped into two basic categories, direct mixing and surface application. This study will address one method from each category. The direct mixing method was modeled after a procedure conducted by (Lei et al., 2006). To assure sufficient mixing, REE oxides were mixed with a small amount of soil and then with the total soil for the layer. The developed surface application method is an adaptation of a method carried out by (Deasy and Quinton, 2010). In this study REE oxide powders were suspended in water and then sprayed on the soil surface with a backpack sprayer. This study was designed to allow for these methods to be tested simultaneously.

4.2.2 **Soil REE Background and Target Concentrations**

These particle labeling methods required the addition of REE oxides to the soil profile to act as the tracer. Since REE are naturally present in most soils, background concentrations of REE in the soil had to be established before tracers could be added. The target concentration of the soil in the plot after tracer application was set to be 10 times that of the background concentration. The experiment called for six REE oxides to be used as tracers in this study. ICPMS analysis of 10 REEs was undergone on three randomly collected soil samples for background concentrations (Table 4.1**).** The six REEs to be used for the experiment were then chosen for the least cost and availability.

Table 4.1: Soil background concentrations of REEs in ppm.

Soil REE Background Concentrations			
Element	Symbol	Oxide	Background [ppm]
Lanthanum	La	La_2O_3	29.39
Cerium	Ce	CeO_2	27.25
Praseodymium	Pr	Pr_2O_3	7.16
Neodymium	Nd	Nd_2O_3	7.64
Samarium	Sm	Sm_2O_3	4.12
Europium	Eu	Eu_2O_3	1.10
Gadolinium	Gd	Gd_2O_3	5.57
Terbium	Tb	Tb_4O_7	0.68
Dysprosium	Dy	Dy_2O_3	3.02
Ytterbium	Yb	Yb_2O_3	1.27

The six REEs chosen for this experiment were Ce, La, Gd, Nd, Sm, and Yb. The REEs for application came in oxide powder. When calculating REE application rates, it was necessary to account for the mass fraction of oxygen in then REE oxide powder. With oxygen mass fraction accounted for, target concentrations of 10 times background concentrations could theoretically be achieved by adding REE oxides to a soil mixture of known mass.

4.2.3 **REE Soil Mixing**

The direct mixing method for tracer application required that the tracer be incorporated evenly to the entire erodible soil layer through mixing. The entire layer of soil must be removed for the mixing process. In this case the soil was mixed with REE tracers before it was placed in the soil bed. The soil bed was divided into six sections, each of which would require a unique REE soil mixture to fill the top layer. Assuming the base layer was level, each of the six top layer section would require the same amount of soil to fill the top layer to a depth of 5 cm. The required soil volume per section was calculated and converted to a mass assuming a soil bulk

density of 1400 kg/m^3. Now that soil mass was known, the amount of REE oxide powder required to bring the soil REE background concentrations to 10 times their natural level could be determined.

The top layer of soil media, which had been sieved and air dried, was put into buckets for preparation of mixing. REE oxide powders were carefully weighed and then added to two liters of dry soil. This mixture was then mixed by hand to assure complete mixing. The total soil and the REE soil mixture were then placed inside of a concrete mixer (Figure 4.7). The concrete mixer stirred the soil mixture for 15 min. A cardboard lid was fastened over the mixer opening to prevent dust from escaping during the mixing process. After mixing the soil media was returned to buckets to await soil bed preparation. This mixing process was carried out six times, once for each REE. Care was taken to prevent cross contamination of REE between soil batches. The concrete mixer was meritoriously swept out after each mixing session, the area was cleared of spilled soil, and the buckets were well labeled to prevent cross contamination. After collection, air drying, sieving, and mixing the soil was finally ready for bed preparation.

Figure 4.7: Concrete mixer dumping REE mixed soil into bucket

4.2.4 **Soil Bed Preparation and REE Surface Spray Application**

The soil bed's base layer was prepared in the manner describe in section 4.1.2. This section specifically details the procedure for top or erodible layer loading and preparation for REE tracing methods. The base layer of soils provided a uniform surface from which the top layer was to be constructed. But first the twin compartments needed to be divided into three equal sections. To achieve this, galvanized steel partitions were placed into the compartments on the section dividing lines**.** Each of the six sections was then filled with an assigned variety of REE mixed soil, see Figure 4.8 for section assignments. The sections were filled individually to a depth of 5 cm in 2 cm lifts. Soil was leveled after each lift with a hand rack and compacted with a tamp. A wooden float was used to smooth the surface of the soil after final compaction.

After final compaction the soil was ready for the second REE application, which was to be topically applied instead of mixed. The REE oxide powders were applied to the soil plots using a hand pump spray bottle while suspended in deionized water. As in the mixing procedure, each section was assigned a specific REE for application (Figure 4.8**)**. A serpentine spray pattern was used to apply the REE solution uniformly over the section area. To keep the REE oxide particles in suspension, the bottle had to be shaken periodically. To prevent overspray, the metal partitions were left in place until all spray applications were completed. The spray bottle was rinsed with deionized water after each section to prevent cross contamination of REEs. The same mass of REE oxide powder was applied to the surface via spray method as had been through direct mixing.

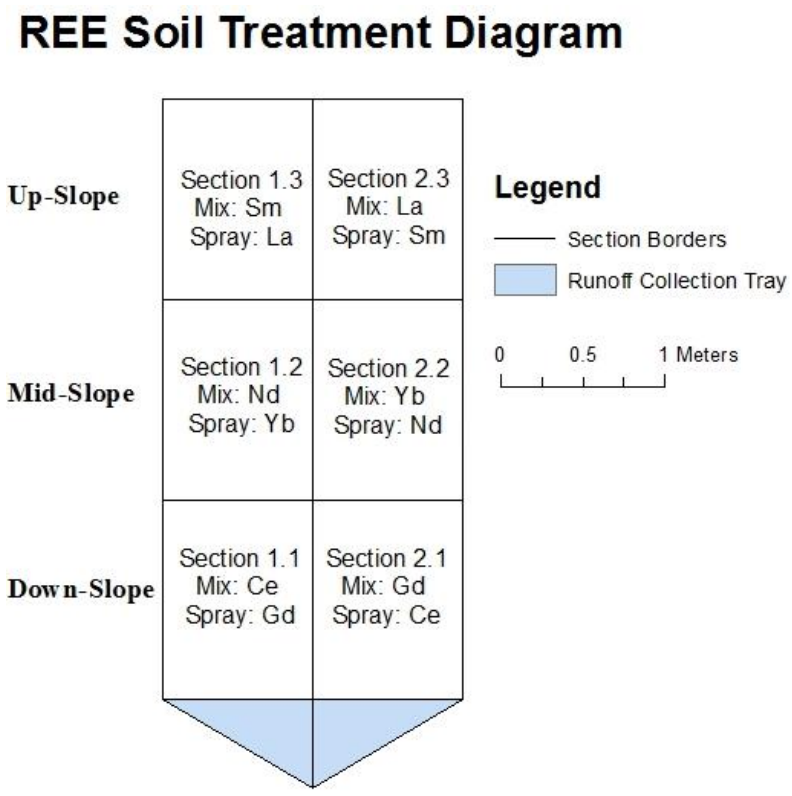

Figure 4.8: Diagram of REE mixing and spray regime

After REE applications were completed the section partitions were removed to reveal one continuous soil plot. At this point the soil in the compartments were brought to saturation and allowed to dry three times over the course of a week. The wetting and drying cycles were intended to help incorporate the REE oxide into the soil aggregates (Mao et al., 2013). Also, wetting and drying the soil encouraged natural settling and compaction. The soil was brought to saturation by running water over the surface. To prevent soil incision during the saturation, the surface of the soil was protected with a fine plastic mesh which dissipated most of the energy of flow. After the final drying cycle the plot was brought to saturation once more and allowed to dry for 24 hours. This was to be the initial antecedent plot condition for REE sediment source tracking experimentation.

4.2.5 **REE Experimental Procedures and Computations**

After plot preparation, REE sediment source tracking trials were undertaken with the use of rainfall simulation. The rainfall simulation procedure was designed to observe the effects of multiple rainfall events on a soil's surface. REEs were used in an attempt to track cumulative effects of rainfall simulation. The erosion plots and rainfall simulator were arranged in the manner presented in section 4.1.3 Rainfall Simulation Overview. The twin plots were subjected to the design storm of 51 mm/hr for a duration of 30 minutes six times. The simulations were performed on 24 hour intervals. The timing was fiercely regulated to ensure similar antecedent plot conditions between trials.

Runoff samples were collected for sediment analysis, and the samples were processed as described in sections 4.1.4 and 4.1.5. All collected samples were analyzed for sediment concentration. Samples collected from the total runoff bucket were combined and analyzed to yield a representative REE concentration. REE computations for sediment source tracking were

modeled after work done by Lie et. al., (2006). Lei preformed a similar sediment source tracking experiment modeling the transport of sediment in rills subjected to overland flow (Lei et al., 2006).

Measuring soil background concentration was the first step in computing the amount of soil eroded from each segment of the plot. This process was taken care of before experimentation began to determine the application rates of REEs to the soil. The second factor needed was to measure the REE soil concentrations after REE mixing/application.

All eroded sediments were captured during rain simulation in plot runoff. For each simulation the total sediment yield, Y_t , was calculated for each plot. Y_t was derived from the measured total sediment concentration and the total runoff volume. Individual REE concentrations, c_i ($i = 1, 2, 3$), were also measured with ICPMS. Zhang et al., (2001) reported that REEs tag similarly across all soil aggregate sizes. With this assumption the tracer enrichment factor was assumed to be one. In other words, the concentration of REEs in the eroded sediments was assumed to be equal to the concentration of REEs in the plot soil after REE application. The eroded amount of applied REE, $e_i(i = 1, 2, 3)$, could then be calculated by subtracting c_i from its corresponding background concentration, $C^o{}_i(i = 1, 2, 3)$, and multiplying by the Y_t.

$$e_i = (c_i - C^o{}_i)Y_t$$

The eroded amount of applied REE, e_i, is also equal to the amount of sediment eroded from each of the three plot sections, $Y_i(i = 1, 2, 3)$, multiplied by the differrance of the concentration of REE after application, $C_i(i = 1, 2, 3)$ and the corresponding $C^o{}_i$.

$$e_i = Y_i(C_i - C^o{}_i)$$

Y_i can then be given as

$$Y_i = \frac{e_i}{(C_i - C^o{}_i)} .$$

With substitution, the Y_i can be written as:

$$Y_i = \frac{(c_i - C^o{}_i)Y_t}{C_i - C^o{}_i} .$$

These computations were performed for both application procedures for all rain simulations.

4.3 Interrupted Rill Method

A less technical method for sediment source tracking is the method of interrupted rills. This method involves measuring sediment yield at intermediate points along a watersheds flow path. By this procedure, nested sub watersheds boundaries are defined and there individual contribution to total watershed sediment yield can be analyzed. Lei et al., (2001) performed an experiment relating sediment transport capacity to rill length. However, Lei's experiment was designed for overland flow (Lei et al., 2001). This section is dedicated to the description of a method which adapts interrupted rill methodology to a rainfall simulation.

4.3.1 Experimental Design

Applying the interrupted rill method to a smaller plot scale environment can present some challenges. The method divides the erosion area into smaller subareas. In larger watershed scale experiments, there would often be naturally fitting areas of concentrated flow which would be suitable for sampling and measuring flow. However, the erosion plots used in these experiments were relatively small (0.75 x 3.6 m), and the soil loaded into the beds was level. At this scale,

points of concentrated flow would not be well defined. Most of the runoff was expected to occur as sheet flow. These factors created challenges with implementing the interrupted rill process.

Since points of concentrated flow could not be well defined, it would be extremely difficult to take samples and to measure flow at intermediate points along the extent of the plot. Even if sampling was possible, it would be difficult to determine exactly which areas of the plot the samples would represent. To solve this problem, the plot need to be artificially divided into manageable, well defined sections. As in the REE trials, the plots were divided into three lateral sections, a top, middle, and bottom. The process of interrupted rills requires runoff sampling and flow measurements at the end of each nested section. To collect a representative sample of the sheet, the entire flow was fenced off at these locations and collected. However by collecting the entire flow at intermediate points, the interaction between different plot sections cannot be accounted for. Erosion and deposition resulting from the upper section flowing over the lower sections would be eliminated in this scenario. To combat this issue the experiment was designed to be carried out in three phases of rainfall simulation, one for each level nesting. The first phase measured the sediment yield originating from the top one third of the erosion plots, the second phase measured sediment yield from the top section and the middle section, and the third phase measured sediment yield from the entire plot **(**Figure 4.9**)**. Performing the experiment in three phases provided information on how the three sections interacted with one another. This method required three times the amount of simulation as the REE method. For efficiency the third phase of the interrupted rill experiment was ran in conjunction with the REE trials. An assumption was made that REE application to the soil did not have an effect on soil erodibility or total plot sediment yield.

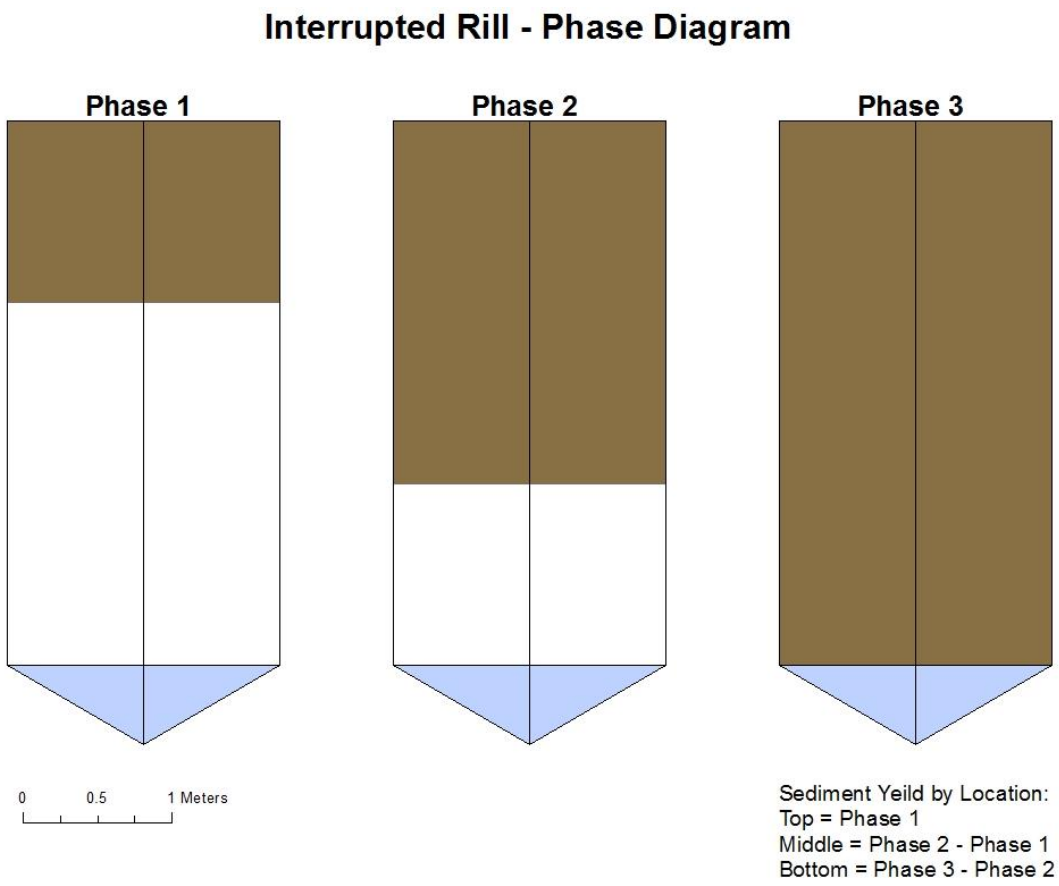

Figure 4.9: Phase area diagram for Interrupted Rill Method

4.3.2 **Interrupted Rill Setup**

As specified in the design, this experiment needed to be carried out in three phases, each with a different plot length. In order to do this, the erosion plot as described in section 4.1.1 Erosion Plot Overview needed to be modified to accommodate phases with shorter plot lengths. The bulk of the erosion plot remained unchanged apart from the addition of a fence, which replaces the front plot border. The fence was constructed out of galvanized steel and fastened to wooden board. Holes were drilled into the steel to allow runoff to pass through the fence in the same fashion as the front plot border. A PVC trough was attached to the outside of the fence to capture runoff (Figure 4.10). The trough directed runoff into a piping system leading to carboy

containers. The fence was clamped in place on the plot dividing lines to create a new plot boarder. After it was secured the edges were sealed with silicone and bentonite was packed around the sides and bottom to ensure a tight seal.

Figure 4.10: Border fence set up during phase 1 experiment

The base layer of soil was prepared for the entire length of the plot as described in section 4.1.2 before the installation of the plot fence. Once the fence was installed, the erodible layer was added. The erodible layer measuring 5 cm in depth was added to the plot on top of the prepared base layer. The erodible layer was removed and reapplied in between trials for consistency. The soil media was prepared and added to the soil compartments in the same

method as in the REE study with a few exceptions. Phases 1 and 2 did not require REE mixing or spray application. Also, since the testing region did not span the entirety of the plot during phases 1 and 2, less soil was needed to prepare the erodible layer. As aforementioned, phase 3 was carried out in conjunction with the REE trials so soil plot preparation was as described in section 4.2.4.

4.3.3 **Interrupted Rill Procedure and Computations**

After plot preparations, the twin plots were ready for rainfall simulations. The twin plots were subjected to six 30 minute design storms of 51 mm/hr, the same simulation conditions as the REE trails. Runoff samples were collected for sediment analysis and samples were processed as described in sections 4.1.4 and 4.1.5. All collected samples were analyzed for sediment concentration. REE concentration was not needed for this analysis.

For this experiment more emphasis was placed on sediment yield and flow rates. The objective of the sediment source tracking experiment was to determine how much soil was displaced from each section and how that related to the total sediment yield, S_3. S_3 was represented by the phase 3 experiment when the total plot length was used. The sediment yields from phase 1 and 2, S_1 and S_2 respectively, were used to determine plot contribution. The contribution of each section, top, middle, and bottom, to the total sediment yield was calculated as follows:

$$top = S_1\ , middle = S_2 - S_1, and\ bottom = \ S_3 - S_2,$$

where,

$$top + middle + bottom = S_3.$$

4.4 Ground Based LIDAR Method

The final method utilized for sediment source tracking in this round of experiments was ground based LIDAR. Ground based LIDAR is an emerging technology, and is beginning to see wide spread use in erosion studies. Vinci et al., (2015) utilized this technology to model rill formation on a hillslope. In this study Vinci scanned the surface of a plot on a hillslope before and after multiple rainfall events. After the rainfall events Vinci et al., (2015) recorded significant sediment movement, which was visible in the formation of rills. Vinci focused most of the study on the formation of rill networks. This technology was adapted in this study to measure the movement of sediment down the slope. This section will explain the methodology of using ground based LIDAR as a sediment source tracking technique.

4.4.1 Ground Based LIDAR Experimental Design and Setup

Ground based LIDAR is a technology that takes surface measurements from a fixed point with a laser. The measurements are stored in a point cloud, whose coordinates are represented in a three-dimensional reference system. From the point cloud, a three-dimensional surface can be rendered from an interpolation program. A surface must be developed before and after each erosion event to quantify the sediment movement associated with said event. In order to take these precise measurements, first the instrument needs to be oriented. The first step is to established fixed points that will not be altered by simulation in the scan area. The first fixed point, the origin, is needed to establish a coordinate system from which successive scans can be oriented. Next, points are needed to define the extent of the scan area, e.g., the plot boundaries. Once the instrument is oriented on these fixed points, the area within the boundaries can be measured. Most ground based LIDAR systems will have a method of measuring the points inside of the boundary. An efficient method is to create a grid (Figure 4.11). The closer grid spacing

will result in a better representation of the surface. Some factor effecting grid spacing are plot size, topography, and instrument specifications.

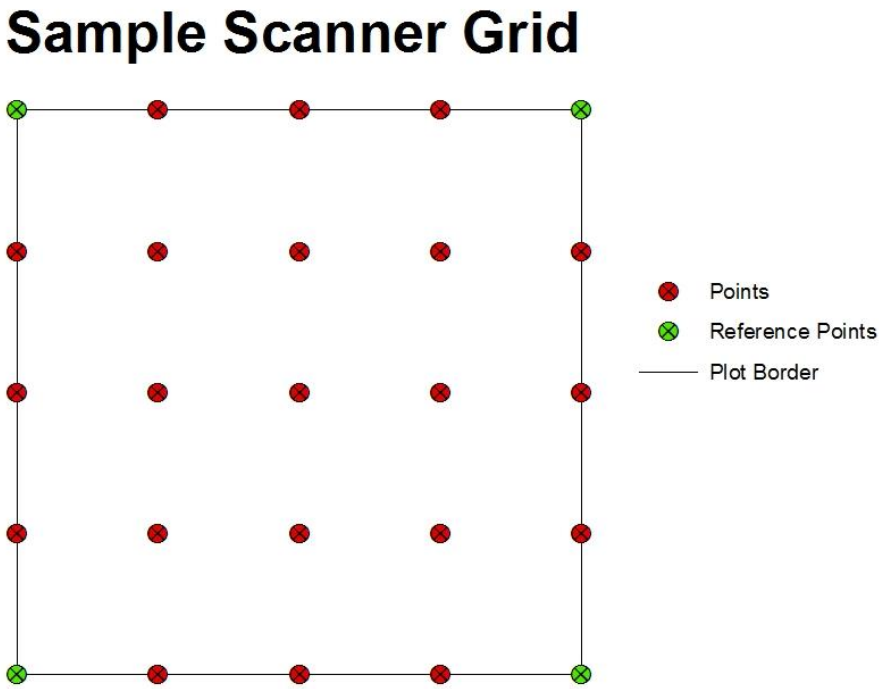

Figure 4.11: Sample scanner grid

This experiment was run in conjunction with the REE trials. All plot setup and simulation procedures were as described in section 4.2 except for the addition of plot reference points (Figure 4.12**)**. The plot reference points were steel bolts anchored 20 cm into the soil media to prevent movement during simulation. The bolt heads were painted white, which made locating the points with the laser easier. The instrument chosen for these experiments was a Lecia 3-D Disto (Figure 4.13). The Lecia 3-D Disto is capable of measuring grids to 1 cm intervals with an accuracy of ± 1 mm in all directions. The instrument is controlled remotely with a wireless handheld device.

The instrument was mounted to a stairway 2 m above and 1 m in front of the plots to provide a proper vantage points for the measurements. Based on previous trials a 2 x 2 cm gridding system was chosen for all scans. Completing a surface scan at 1 x 1 cm took almost twice the time as a 2 x 2 cm scan. Also, scans measured at 1 x 1 cm were not determined to be significantly superior to scans of 2 x 2 cm.

A total of six rainfall simulations were carried out over the erosion plots. In order to monitor sediment movement across the plot, a total of seven surface scans were taken, one before simulation and one after each subsequent rainfall simulation. This scanning procedure was carried out for both plots 1 and 2. The point clouds for each scan were temporally stored in the Leica handheld device before being uploaded to a computer for post processing.

Figure 4.12: Plot set up for Ground Based Lidar

Figure 4.13: Leica 3-D Disto mounted above erosion plots

4.4.2 **Data Processing and Computations**

Once the point clouds have been uploaded to a computer, post processing could begin. The Leica 3-D Disto creates multiple files loaded with a myriad of information. The only information needed for 3-dimensional surface creation are the 3-dimensional, (x,y,z), coordinates stored in the point cloud. The data was transferred to Microsoft Excel, a platform from which each point was condensed to a basic 3-dimensional coordinate. Each surface scan was comprised of approximately 6500 points. The condensed list of points was saved in Excel as a comma separated variable (.csv) file, a file compatible with most interpolation software.

Two software programs were chosen to create 3-dimensional surfaces, Surfer (version 10.1.561) and ArcMap (version 10.2.1). Each tool used a gridding method based off of Kriging interpolation, a common interpolation in geostatistics. The Kriging method is based on

regionalized variable theory, assuming spatial variation in that data is consistent across the surface. An example of a Kriging generated surface generated by the surfer program is shown in Figure 4.14.

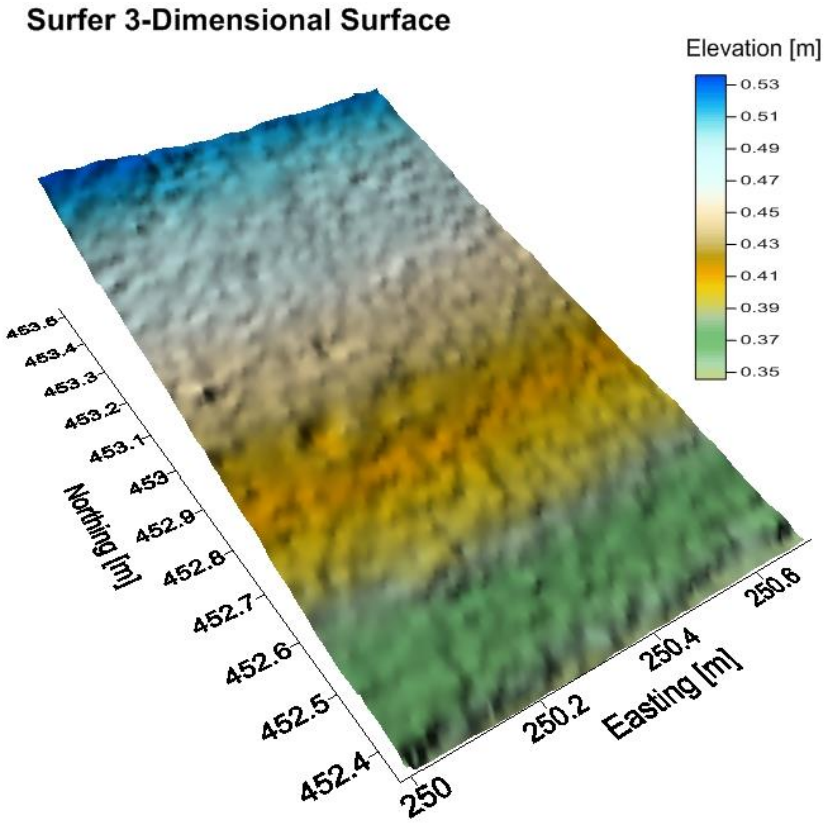

Figure 4.14: 3-D surface constructed in Surfer

Each total surface was divided into three subsections, top, middle, and bottom. Since every simulation's surface had a common coordinate system, surfaces could be overlain for cut and fill volume calculations. Surfer calculated cut and fill volumes between various surfaces with the trapezoidal rule. The addition of negative cut and positive fill measurements between surfaces would indicate the total sediment movement of said erosion event/events. A net

positive volume would indicate soil gain (deposition) and a net negative volume would indicate soil loss (erosion).

Chapter 5

Results and Discussion

5.1 Rainfall Characteristics

The initial measured UC for the total plot areas was 0.83. The suggested acceptable UC for rainfall simulators is 0.80 (Huffman et al., 2011). Despite the acceptable UC, the simulator still exhibited some areas of concentrated or insufficient rainfall (Figure 5.1**)**. The UC was calculated for plots 1 and 2 separately yielding UCs of 0.80 and 0.89 respectively (Table 5.1). The inconsistent rainfall patterns observed in plot 1 suggested a need for simulator calibration. Adjustments were made to the rainfall simulator to improve the UC. Nozzle oscillation and output was held constant. The adjustments were made to the trough gaps through which nozzle spay passes. Larger trough gaps allowed more water to pass than smaller trough gaps. Adjustable diversion pans were placed over the trough gaps to control trough gap size.

After nine adjustments to the diversion pans and subsequent simulations, the total plot UC plateaued at 0.91. The individual plots 1 and 2 UCs reached 0.90 and 0.93 respectively. This configuration was considered acceptable since further adjustments to the diversion pans produced diminishing returns on the UC. Further improvements to the UC would require extensive rainfall simulator modification which was not considered practical for the purposes of this study.

During this calibration, more emphasis was placed on rainfall uniformity as opposed to average rainfall intensity. The rainfall simulator had been previously calibrated for intensity for the use in other studies. The target storm intensity for the simulation was 51 mm/hr. After adjustments were made the average storm intensity produced by the simulator was measured to

be approximately 55 mm/hr with plot 1 receiving slightly heavier precipitation than plot 2 (Table 5.1**)**. Even though the rainfall intensity measured slightly higher than the target rate, it was accepted because it remained consistent between trials.

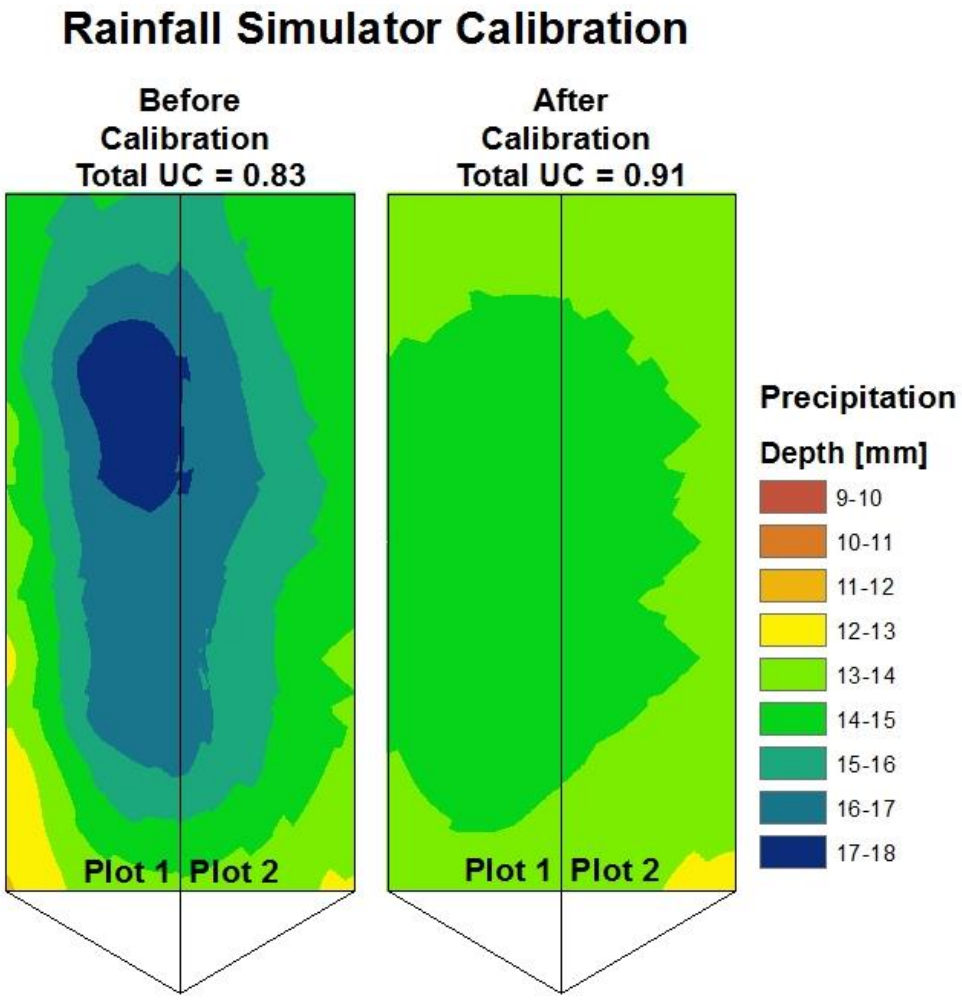

Figure 5.1: Rainfall distributions over plot surfaces before and after uniformity calibration

Table 5.1: Average rainfall intensity and UC for plot areas before and after uniformity calibration

Before Calibration				After Calibration		
Area	Intensity [mm/hr]	Uniformity Coefficient		Area	Intensity [mm/hr]	Uniformity Coefficient
Plot 1	59.90	0.80		Plot 1	56.40	0.90
Plot 2	58.60	0.89		Plot 2	53.50	0.93
Total	58.24	0.83		Total	54.84	0.91

5.2 REE Particle Labeling

The use of REE material as a tracer for studying sediments movement is not a new theory. The development of and widespread availability of small particle analysis technologies such as ICPMS has kept scientists interested in the subject since the 1980s. Literature suggests a lack consensus amongst researchers on proper REE and soil preparation procedure. No research has been done comparing the effects of various methods. The following section highlights some of the challenges associated with the REE labeling methods and their ability to predict sediment sources.

5.2.1 REE Background and Post Application Measurements

Soil background concentrations were necessary to develop baseline concentrations for REE application procedures. Six REEs were chosen for this experiment on the basis of material cost and availability. The six REEs chosen for the experiment are shown in Table 5.2 with their respective background concentrations.

Table 5.2: Comparison of measured REE background concentrations with literature

Soil REE Background Concentrations [PPM]

Researchers	Location	Soil Type	Ce	Nd	Sm	Gd	Yb	La
Schumacher	Urbana, IL	Silty Clay Loam	27.25	7.64	4.12	5.57	1.27	29.39
Zhang et al. 2003	West Lafayette, IN	Silt		16.29	3.18	2.98		17.06
Zhu et al. 2011	Danjiangkou, China	Silty Clay	33.05	22.54	3.17		2.35	21.4
Lie et al. 2006	Loess Plateau, China	Silt Loam	66.1	31.1	5.8		2.64	35.4

Of the background concentrations lanthanum was reported to have the highest concentration at 29.39 PPM, and ytterbium was reported to have the lowest concentration of 1.27 PPM. These values are supported by values obtained from literature as noted in the table. Background concentrations were consistently low in all the studies listed despite drastic changes in sample locations. To put these numbers in perspective total quantitative analysis of all elements up until atomic number 92 was run on the background samples. Some of the results are listed in Table 5.3.

Table 5.3: Background concentrations of other notable elements in comparison to REEs

Other Notable Elements

Element	Concentration [PPM]
Al	47138.23
Fe	28410.61
K	8083.65
N	1376.02
P	514.68
Pb	18.31
U	4.23
Hg	0.25

REEs

Element	Concentration [PPM]
Ce	27.25
Nd	7.64
Sm	4.12
Gd	5.57
Yb	1.27
La	29.39

REEs were present in the soil at nearly the same levels as elements such as Pb and U. These concentrations are several orders of magnitude less than key soil nutrients N, P, and K. The background testing proved that REEs are in fact present in the soil. These "rare" elements are not as rare as they are made out to be. In fact, of the 92 elements tested for in the total quantitative analysis, all but eight were accounted for in all least some trace amount.

After background concentrations were determined, the soil mass was tagged with REO powders as described in the methodology in an attempt to achieve the desired target concentrations of 10 times the background concentration. Once the soil plots were prepared, surface soil samples were taken to determine the new REE concentrations of the source materials. The results for both REE application methods, mix and spray, are represented in Table 5.4 and Table 5.5 respectively.

Table 5.4: Measured concentrations of REE after mix application. Factor represents measured concentration divided by background concentration.

Mixing Application Concentration [PPM]

Section	REE	Background	Measured	Factor
1.1	Ce	27.25	46.68	1.71
1.2	Nd	7.64	40.37	5.28
1.3	Sm	4.12	13.19	3.20
2.1	Gd	5.57	60.53	10.87
2.2	Yb	1.27	5.89	4.65
2.3	La	29.39	36.63	1.25

Table 5.5: Measured concentrations of REE after spray application. Factor represents measured concentration divided by background concentration.

Spray Application Concentration [PPM]

Section	REE	Background	Measured	Factor
1.1	Gd	5.57	416.10	74.74
1.2	Yb	1.27	5.26	4.15
1.3	La	29.39	35.84	1.22
2.1	Ce	27.25	148.20	5.44
2.2	Nd	7.64	48.75	6.38
2.3	Sm	4.12	15.11	3.67

REO powder was added to the erosion plots in sufficient quantities to theoretically raise soil REE concentrations to 10 times their natural background concentration. The measured concentrations of REEs in the soil after application are displayed alongside the original background concentrations. After REE application, it is evident that tracer REE concentrations increased over their aforementioned background concentrations for both application methods. However, the multiplicative factor of concentration increase is not consistent across the spectrum of selected tracer elements for either application method.

The target factor of increase was 10. With the exception of Gd, all other factors measured much lower than 10. This leads to some concerns about homogeneity of tracer bonding to the soil media. The tracer was applied to achieve desired concentration. For the most part this concentration was not achieved, which leaves a portion of the applied tracer unaccounted for. This suggests that the tracer may not have bonded to the soil media as homogeneously as intended. A portion of the tracer may not have bonded to the soil and be present in the soil as a free particles.

The same amount of each tracer was applied to the plots in each application method. Even though a 10 times increase in tracer concentration was not achieved, it is interesting to note

that most individual elements were recovered in similar concentrations from both mix and spray applications. For example the factor of Sm for mix application is similar to the factor of Sm for spray application. This affinity between applications methods suggests that REO powders may react similarly to soils regardless of application method. Since the factors are not consistent between REEs, there is also an indication that some REO powders may be more conducive to soil homogeneity than others.

5.2.2 **REE in Eroded Sediments**

All runoff was collected from each simulation. Runoff volume and sediment concentrations were recorded and calculated to be used in sediment yield calculations. The simulation sediment yields for each plot are displayed in Table 5.6**.**

Table 5.6: List of plot sediment yields [g] in reference to simulation number

Total Plot Sediment Yield

Simulation	Plot 1 [g]	Plot 2 [g]
Rain 1	693.12	534.44
Rain 2	775.90	566.93
Rain 3	743.20	561.33
Rain 4	629.44	611.09
Rain 5	737.06	565.87
Rain 6	596.58	556.61
Mean	695.88	566.04

The sediment yields for plot 1 and 2 are similar between simulations. The standard deviation for plots 1 and 2 are 70 and 25 gram respectively and for both plots there is little correlation between simulation number and sediment yield. These factors suggest that each simulation is eroding the soil at approximately the same rate. Plot 1 consistently measured higher in total sediment yield than plot 2 resulting in a mean sediment yield difference of almost 130 g. Assuming a soil bulk density of 1.4 g/cm^3, the average soil volume eroded from plots 1

and 2 are 497 cm^3 and 397cm^3 respectively. The higher sediment yields in plot 1 were probably a result of the slightly higher rainfall intensity recorded over plot 1 (Figure 5.1). Refer to section 5.3 Interrupted Rills for a more extensive analysis of plot sediment yield.

The eroded sediment from the total bucket runoff samples were also analyzed for sediment concentration. Since both application methods were being tested in conjunction, each sample needed to be analyzed for six REEs. Three for the spray application and three for the mix application. The results for runoff REE concentrations are displayed in Table 5.7 and Table 5.8.

Table 5.7: Concentration of REEs in runoff samples associated with the mixing application. Linear regression for each REE relating simulation number to REE concentration. Slope (m) and coefficient of determination (R^2)

Mixing Application		Concentration [PPM]								
Section	Element	Measured	Rain 1	Rain 2	Rain 3	Rain 4	Rain 5	Rain 6	m	R^2
1.1	Ce	46.68	56.64	57.97	54.60	34.05	41.15	47.77	-3.30	0.42
1.2	Nd	40.37	69.76	80.72	88.93	77.64	75.00	95.11	2.81	0.32
1.3	Sm	13.19	19.58	32.93	31.54	28.56	33.18	35.77	2.50	0.54
2.1	Gd	60.53	57.56	60.29	48.44	42.82	46.98	46.03	-2.95	0.63
2.2	Yb	5.89	111.60	117.40	113.50	95.30	90.41	77.95	-7.64	0.84
2.3	La	36.63	36.16	47.76	44.03	50.13	63.32	61.46	5.12	0.85

Table 5.8: Concentration of REEs in runoff samples associated with the spraying application. Linear regression for each REE relating simulation number to REE concentration. Slope (m) and coefficient of determination (R^2)

Spray Application		Concentration [PPM]								
Section	Element	Measured	Rain 1	Rain 2	Rain 3	Rain 4	Rain 5	Rain 6	m	R^2
1.1	Gd	416.10	188.40	211.60	151.40	163.10	146.80	145.80	-11.31	0.63
1.2	Yb	5.26	601.40	675.70	592.90	672.40	522.20	484.50	-27.59	0.44
1.3	La	35.84	147.60	153.10	110.50	146.90	157.20	177.80	5.71	0.24
2.1	Ce	148.20	94.25	204.40	125.00	87.58	107.90	91.25	-9.77	0.17
2.2	Nd	48.75	304.13	495.50	451.30	409.40	305.30	332.60	-13.43	0.10
2.3	Sm	15.11	85.88	137.80	145.90	161.00	204.60	198.70	22.27	0.91

The first thing to consider when looking at the results are some of the basic assumptions made for this experiment. Most notably, this experiment is based on the assumption that the concentrations of REE in the eroded sediment will be equal to that of the sediments source material. Each plot has three source materials, soil from the top, middle, and bottom. Each source material has been tagged with two REEs, one from the mixing method and one from the spraying method. The assumption is that any sediment exiting the plot should have the same REE concentrations as its source material. Since all three sources are interconnected, sediment from all three sections should be expected to erode and be transported off the plot. The eroded sediment collected in the bucket is then a representation of sediment from all three sources.

With all three sources mixed together, the composite sediment REE concentrations in the bucket should be less than that of the source material. They should be linearly proportional to the amount of sediment present form each source (reference Section 4.2.5). Upon first glance at REE concentrations from the eroded sediments, it is immediately noticeable that many of the eroded sediment concentrations are higher than the measured source concentrations. This realization immediately disproves the essential aforementioned assumption. This is a result of significant tracer enrichment in the eroded sediments.

Tracer enrichment can be represented as the ration between the runoff REE concentration minus background and the measured source concentration minus background:

$$\frac{c_i - C^o{}_i}{C_i - C^o{}_i}.$$

If the assumption was true, this ratio would be equal to the ratio of the sediment yield from the corresponding source section and the total sediment yield (reference Section 4.2.5). The calculated sediment yields according to the method are listed in Table 5.9 and Table 5.10.

Table 5.9: Calculated mixing application sediment yields [g] of source sections per simulation event.

Mixing Application			Calculated Sediment Yield, Y_i [g]					
Section	Plot #	Element	Rain 1	Rain 2	Rain 3	Rain 4	Rain 5	Rain 6
1.1	1	Ce	1048.424	1226.745	1046.136	220.2866	527.2846	630.0428
1.2	1	Nd	1315.514	1732.441	1845.843	1346.183	1516.908	1594.331
1.3	1	Sm	1181.49	2464.742	2246.946	1696.184	2361.68	2081.913
2.1	2	Gd	505.5606	564.4579	437.856	414.1833	426.3688	409.7646
2.2	2	Yb	12757.16	14244.18	13629.77	12431.73	10913.29	9234.099
2.3	2	La	499.7606	1438.099	1134.817	1750.049	2651.045	2464.689

Table 5.10: Calculated spraying application sediment yields [g] of source sections per simulation event.

Spray Application			Calculated Sediment Yield, Y_i [g]					
Section	Plot #	Element	Rain 1	Rain 2	Rain 3	Rain 4	Rain 5	Rain 6
1.1	1	Gd	308.6856	347.8553	246.2167	265.9704	238.4503	236.7619
1.2	1	Yb	104194.9	117094.9	102719.1	116521.9	90444.21	83898.74
1.3	1	La	12697.12	13287.87	8712.255	12621.93	13728.24	15940.86
2.1	2	Ce	296.0518	782.7699	431.9264	266.5792	356.3669	282.7958
2.2	2	Nd	3854.441	6342.297	5767.686	5222.976	3869.651	4224.558
2.3	2	Sm	3976.242	6501.3	6895.233	7629.6	9750.027	9463.088

Based on the Y_i values high tracer enrichments have obviously taken place during the course of this experiment. The values for individual section sediment yield are supposed to add up to the total plot sediment yield for each simulation (Table 5.6). The percent of method overestimation is represented in Table 5.11.

Table 5.11: Percentage of method overestimation from measured sediment yields

	Mixing Application		Spray Application	
Simulation	Plot 1 [%]	Plot 2 [%]	Plot 1 [%]	Plot 2 [%]
Rain 1	511.5153	2575.122	16909.09	1520.608
Rain 2	699.0496	2865.722	18861.11	2549.654
Rain 3	691.4625	2708.29	16112.25	2450.2
Rain 4	518.3451	2388.529	18670.55	2454.749
Rain 5	597.7627	2472.407	15063.84	2615.083
Rain 6	721.8344	2175.429	14438.48	2614.035
Mean	623.33	2530.92	16675.89	2367.39

To properly compare the results from the mixing and spray application procedures, mixing plot 1 should be compared alongside spray plot 2 and mixing plot 2 should be compared with spray plot 1. This is based off of the REE application assignments, e.g., it would be most proper to compare spray Gd with mixed Gd. With this comparison it is easy to see that the tracer enrichment was much more profound in the spray application method. This is probably due to the limited interaction the tracer has with the soil due the application procedure. The tracer is only exposed to the surface of the soil. As a result the tracer may bind to the immediate surface layer of soil in higher than targeted concentrations. In contrast, the mixing method allows for the tracer to come in contact with the entirety of the erodible layer. With less interaction, a spray applied tracer also has less opportunity to bind with soil particles. That leaves free, unbound tracer on the surface of the soil and susceptible to entrainment by runoff. Tracer enrichment has created some serious challenges for this method of sediment source tracking.

Fine sediment enrichment may play a role in the tracer enrichment phenomenon. Fine sediment enrichment occurs during surface erosion when fine grained particles are transported at higher proportions than coarse grained particles. This leads to an eroded sediment material with a finer texture than the source material. Because of the higher surface area per unit mass, fine

grained particles may also have an advantage when it comes to tracer binding. Enrichment is more likely to occur during low energy interrill processes where fine grained particles and unincorporated tracer are more likely to be transported than coarse grained particles. During higher energy rill erosion, coarse sediments are more likely to be transported along with the fines reducing the chance of enrichment.

The design of this experiment was heavily influenced by work accomplished by Lie et al., (2006). Lie did not report significant tracer enrichment in his experiment and was able to calculate sediment yields to within 15% error of measured sediment yields. Lie's experiment used overland flow in a rill where large amounts of sediment were eroded (Lei et al., 2006). This experiment was conducted under a rainfall simulator on an evenly sloping plot, both of which are conditions favorable for interrill erosion which may have resulted in enrichment.

Polyakov et al., (2004) conducted a similar REE tracer experiment under rainfall simulation. As in this experiment, Polyakov noticed that the REE method overestimated plot sediment yield. To remedy this problem Polyakov developed a correction factor in a separate experiment which related measured sediment yield to the sediment yield calculated with the REE method. The correction factor was applied to all REEs with some success (Polyakov and Nearing 2004). However, a single correction factor assumes that all REEs had the same enrichment potential which was not supported by this experiment's test results.

The data from this experiment suggests that some tracers had much higher enrichment ratios than others. This is especially noticeable with Yb, which was present in much higher concentrations in the eroded sediment than it was in the source sediment. If each REE does in fact bind to the soil differently, then a correction factor could be determined for each REE. The correction factor would also have to be validated across application methods. The development

of these correction factors would require many additional simulations and lab testing fees. This additional work was not in the original scope of the project.

Despite the trouble with tracer enrichment, this method still provides some useful information about sediment movement on the plots. By looking closer at these results, it is easy to notice trends in the REE runoff concentrations presented earlier in Table 5.7 and Table 5.8 . Some of the concentrations clearly seem to be increasing or decreasing as simulations progress. To test this, the concentrations were fitted to a simple linear regression. The slope (m) and coefficient of determination (R^2) are listed in the table for each regression.

The first thing to notice are the slopes of the regression lines. Lines with large slope indicate that the concentrations changed drastically over time. For example, reference Nd in spray application with a slope of 22.27 with a stronger coefficient of determination, 0.91. Nd's concentration starts out at 85 PPM and rises to about 200 PPM by the end of Rain 6. Notice that most of the largest slopes are present in the spray application experiment. This is indicative of tracer movement across the plots and greater enrichments. Next, there is a noticeable pattern in the sign of the slope coefficient. The sign is indicative of a positive or negative correlation between the concentration values.

All sections labeled either 1.1 or 2.1 (bottom sections) are negatively correlated, suggesting a decrease in sediment yield contribution over time. Conversely, all plots labeled with a 1.3 or a 2.3 (top sections) are positively correlated, suggesting an increase in sediment yield contribution over time. These correlations suggest that sediment from the top sections may take more time to reach the outlet than sediment form the bottom sections. Sediment leaving the bottom section will be collected immediately by the runoff collection system. However, sediment

leaving the top two sections has two options, it can be transport completely down the slope and exit the plot, or it can be redeposited on a lower section.

After one simulation, in addition to its own sediments, the bottom section will have sediments deposited from the top and middle sections. As a result a mixture of original bottom and newly redeposited top and middle sediments will be eroded form the bottom location during the subsequent simulations. During the subsequent simulations, the top section will continue to erode. These processes will lead to an increase in top sediment concentration and a decrease in bottom sediment concentration. Sediment eroded from the top sections is gone for good and cannot be replaced. On the other hand, sediment eroded from the bottom section has the potential to be replaced by redeposited top sediments. This may eventually cause the top sections to have a higher net sediment loss than the lower sections.

5.3 Interrupted Rills

The second method for sediment source tracking evaluated in this study was the method of interrupted rills. This method consisted of three phases of simulation, each with a distinct plot length. The total erosion plot length is 3.6 m. Phase 1 represents one third the total plot length, phase 2 represents two thirds the total plot length, and phase 3 represents the total plot length. A key assumption in the in these experiments is that each experimental run under different plot lengths follows the same erosion and sedimentation processes. This is fundamentally different from the REE and Ground Based LIDAR methods, which take measurements of erosion and sedimentation with one sampling attempt.

5.3.1 Interrupted Rill Sediment Yield

The Interrupted Rill Method requires the collection of runoff volume and sediment concentration for all simulations in all phases. The average runoff volumes and standard deviations from all six simulations for all three phases are summarized in Table 5.12 below.

Table 5.12: Summary of simulation average phase runoff volumes

Phase Runoff Volume [L]

Plot 1	Mean	Stdev
Phase 1	23.59	0.73
Phase 2	49.67	0.57
Phase 3	71.86	4.39

Plot 2	Mean	Stdev
Phase 1	20.67	0.63
Phase 2	43.57	1.31
Phase 3	65.81	3.85

Plot runoff volume is highly proportional to plot length. Phase 3 represents the total plot length and therefore the total runoff volume. Phase 1, which represents one third of the total plot length, received 33% of the total runoff volume in plot 1 and 31% of the total runoff volume in plot 2. Phase 2, which represents two thirds of the total plot length, received 69% of the total runoff volume in plot 1 and 66% of the total runoff volume in plot 2. Based on the low standard deviations, it can be concluded that variation in plot runoff volume between simulations was also minimal. The greatest variation for all phases can be seen in the first rain event when runoff volumes were much lower (Figure A.2 and Figure A.3). A possible explanation is that soil surfaces were rougher during the first rainfall simulation, resulting in higher infiltration rates due to ponding.

From the rainfall simulator calibration, the average simulation intensity for plot 1 and plot 2 was 56.4 and 53.5 mm/hr respectively. At these rates, a 30 min simulation applied over a plot area of 2.7 m^2 would yield rainfall volumes of 76.14 and 72.26 L for plot 1 and plot 2

respectively. Using the phase 3 average runoff volumes, the soil infiltration was calculated. For plot 1, 5.63% of the rainfall infiltrated the soil surface at an average rate of 1.59 mm/hr. For plot 2, 8.88% of the rainfall infiltrated the soil surface at an average rate of 2.38 mm/hr.

Sediment concentration was also taken into to consideration for sediment yield assessment. The average runoff sediment concentrations and standard deviations from all six simulations for all three phases are summarized in Table 5.13 below.

Table 5.13: Summary of simulation average runoff sediment concentrations

Phase Sediment Concentration [mg/L]

Plot 1	Mean	Stdev		Plot 2	Mean	Stdev
Phase 1	10932.52	966.54		Phase 1	7923.28	670.38
Phase 2	10384.78	1707.55		Phase 2	10857.94	896.11
Phase 3	9180.59	954.76		Phase 3	8272.64	370.24

The average runoff sediment concentrations trended lower in plot 2 than in plot 1. These two factors will lead to a lower sediment yield in plot 2. Again, the most variation in sediment concentration occurred in the first simulation (Figure A.4 and Figure A.5). Higher sediment concentrations near the beginning of sedimentation experiments should be expected due to the initial first flush of easily detached and transported fine sediments.

From runoff and sediment concentrations, sediment yield was calculated. The results are presented by simulation event in Figure 5.2 and Figure 5.3 and summarized in Table 5.14.

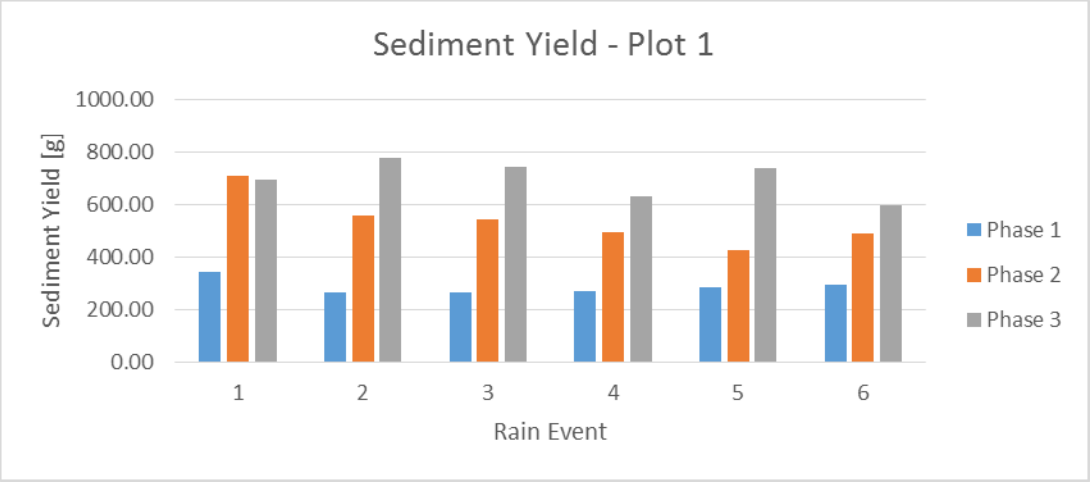

Figure 5.2: Plot 1 sediment yield for each phase of the Interrupted Rill Method. Sediment yield derived from measured sediment concentrations and known runoff volumes.

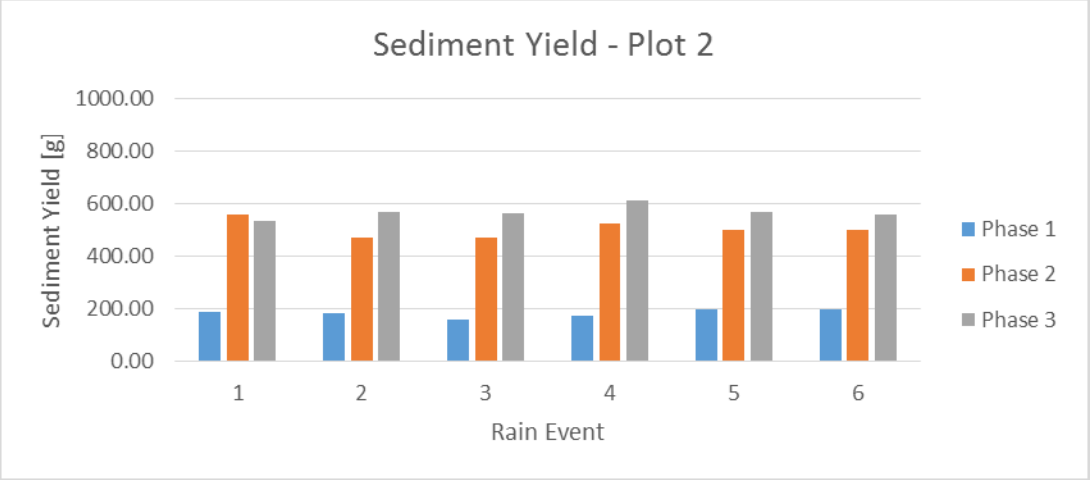

Figure 5.3: Plot 2 sediment yield for each phase of the Interrupted Rill Method. Sediment yield derived from measured sediment concentrations and known runoff volumes.

Table 5.14: Summary of simulation average runoff sediment yields

Phase Sediment Yield [g]

Plot 1	Mean	Stdev
Phase 1	287.12	30.44
Phase 2	535.63	96.36
Phase 3	695.88	70.17

Plot 2	Mean	Stdev
Phase 1	182.88	16.13
Phase 2	504.24	34.93
Phase 3	566.04	25.06

As expected from the runoff and sediment concentration results, the sediment yields from plot 1 trends higher than plot 2. Plot 2 had much more consistent sediment yields between simulations. The highest variation from the mean plot sediment yield occurred during the first rainfall simulations. It was obvious from visual inspection that antecedent soil plot conditions before simulation event 1 were different from the subsequent simulations for all phases. The soil surface was coarse before experimentation, which lead to higher infiltrations and higher sediment detachments. These trends were supported by the results. Surface smoothing as a result of sediment detachment and movement filling in micro-depressions was visible after the first simulation.

Assuming unique plot areas of phases 1, 2, and 3, Table 5.15 expresses average sediment yield as kg/ha.

Table 5.15: Average sediment yields [kg/ha]

Sediment Yield [kg/ha]

	Plot 1	Plot 2
Phase 1	3190.25	2031.947
Phase 2	2975.7	2801.321
Phase 3	2577.341	2096.462

From the perspective of soil conservation in agricultural soils, tolerable erosion (T) is generally considered to be between 5000 and 12000 kg/ha/yr (Schertz, 1983). These T values were exceeded after just a few simulations. Soils in these conditions would certainly require BMP implementation to bring loss within reasonable limits.

In order to apply this knowledge as a sediment source tracking technique phase subtractions were carried out in accordance with the methodology. The results are presented in Figure 5.4 below.

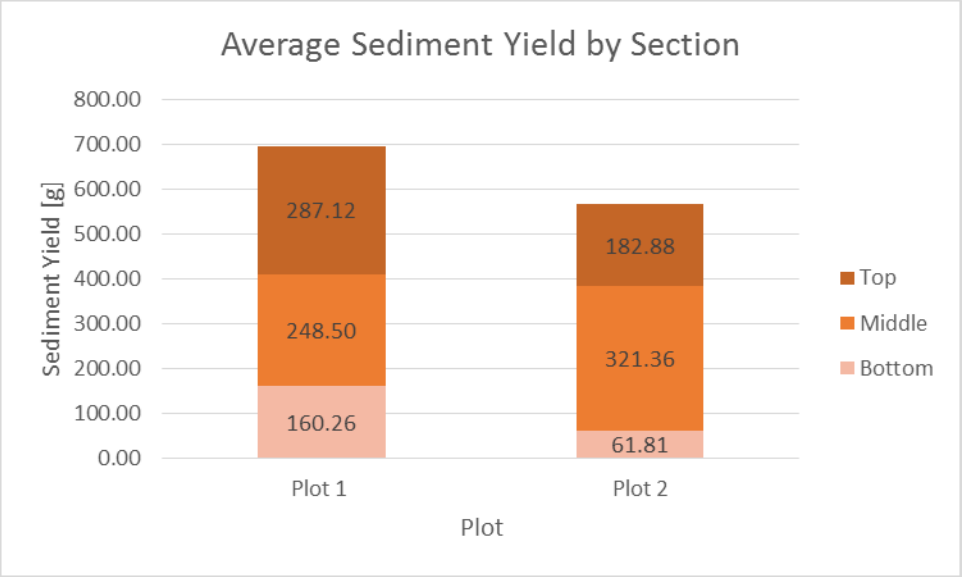

Figure 5.4: Average sediment yield by section. Derived through phase subtractions in Interrupted Rill Method.

The results show that from plot 1 41.26%, 35.71%, and 23.03% of the total soil displacement was eroded from the top, middle and bottom sections respectively. From plot 2, 37.20%, 65.36%, and 12.57% of the total soil displacement was eroded from the top, middle, and bottom sections respectively. This suggests that the greatest net soil displacement in plot 1 was the top section and from plot 2 was the middle section. For both plots, the bottom section shows the least net soil displacement. This is consistent with the theory form the REE trials that significant amounts of deposition is occurring in the lower sections, reducing net contribution to sediment yield.

5.4 Ground Based LIDAR Method

The final sediment source tracking technique evaluated in this study was ground based LIDAR. This study was conducted in conjunction with the REE trials and phase 3 of the Interrupted Rills Method. Unlike the Interrupted Rills Method, this method required on one phase of simulations to make measurements for sediment source tracking. A Lecia 3-D Disto laser scanner was used to make measurements of the entire plot surface as described in the methodology.

5.4.1 Erosion and Deposition Patterns

DEMs constructed with data obtained by scanning the soil surface between simulations were used to measure net soil loss. Surface smoothing and soil compaction resulting from rainfall was observed during the first rainfall simulation. Rain drop impacts dispersed soil aggregates, which increased surface soil bulk density. In addition, settling of deeper soil layers may have occurred because of water movement and percolation. The smoothing and settling caused this method to drastically overestimate soil loss in the first rain. For the purposes of this analysis, the first rain event was ignored and analysis started after the second rain event when plot surfaces had settled. The surface scan after the first rain event was used as a baseline to reference sediment movement from that point on.

Both inter-rill and rill erosion occurred on the plots. Visible rills were present after the first simulation and continued to develop as simulations progressed. The histograms in Figure 5.5 and Figure 5.6 show the frequency distribution of soil loss depth in relation to rain event. In both figures, the frequency distribution of soil loss depths shifts to the right (deeper soil loss). In addition, the range of soil loss increased. This trend suggests that inter-rill erosion dominated

the first few rounds of simulation. As simulations progressed flow accumulated, incising rills into the plot making rill erosion increasingly prevalent.

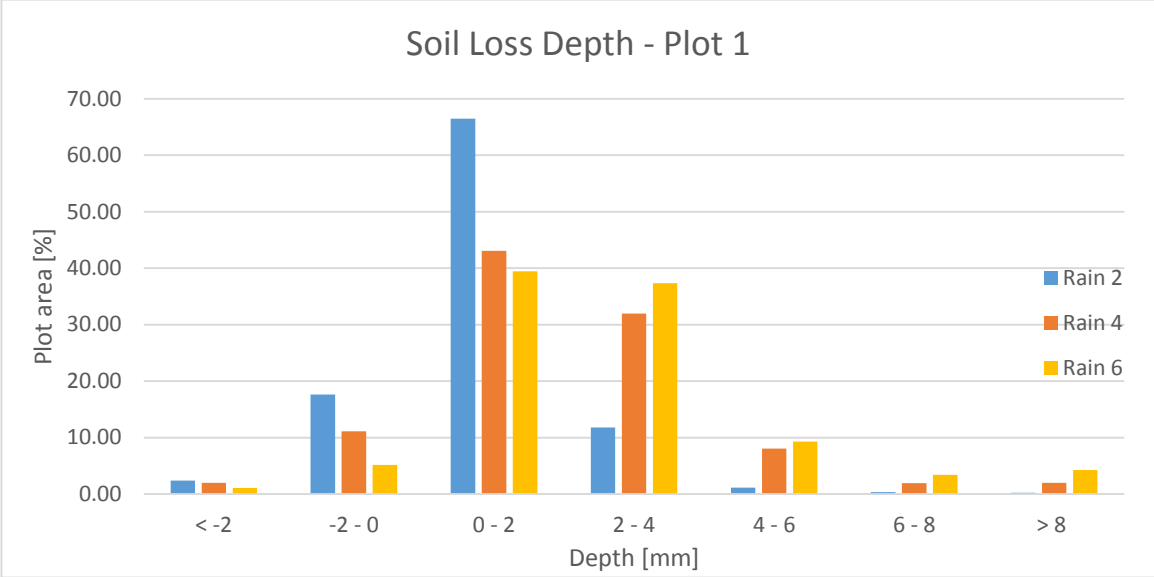

Figure 5.5: Progressive plot 1soil loss depths in reference to Rain 1 DEM

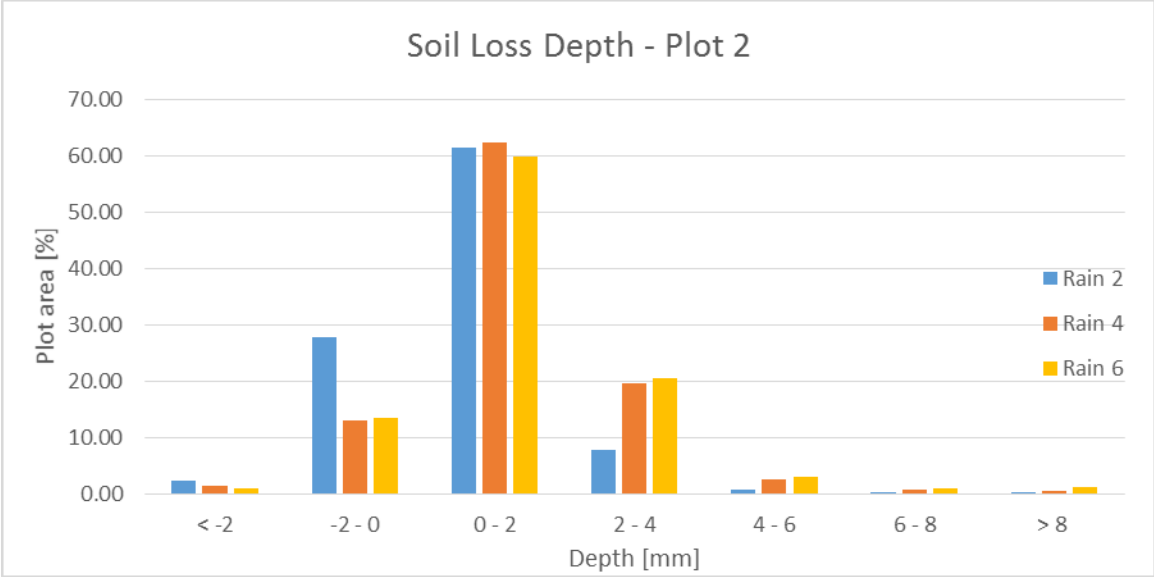

Figure 5.6: Progressive plot 2 soil loss depths in reference to Rain 1 DEM

The DEMs used to create the histograms above are shown below in Figure 5.7 and Figure 5.8. These figures prove that soil erosion is a spatially variable process. Areas of rill formation and deposition are easily displayed with DEMs.

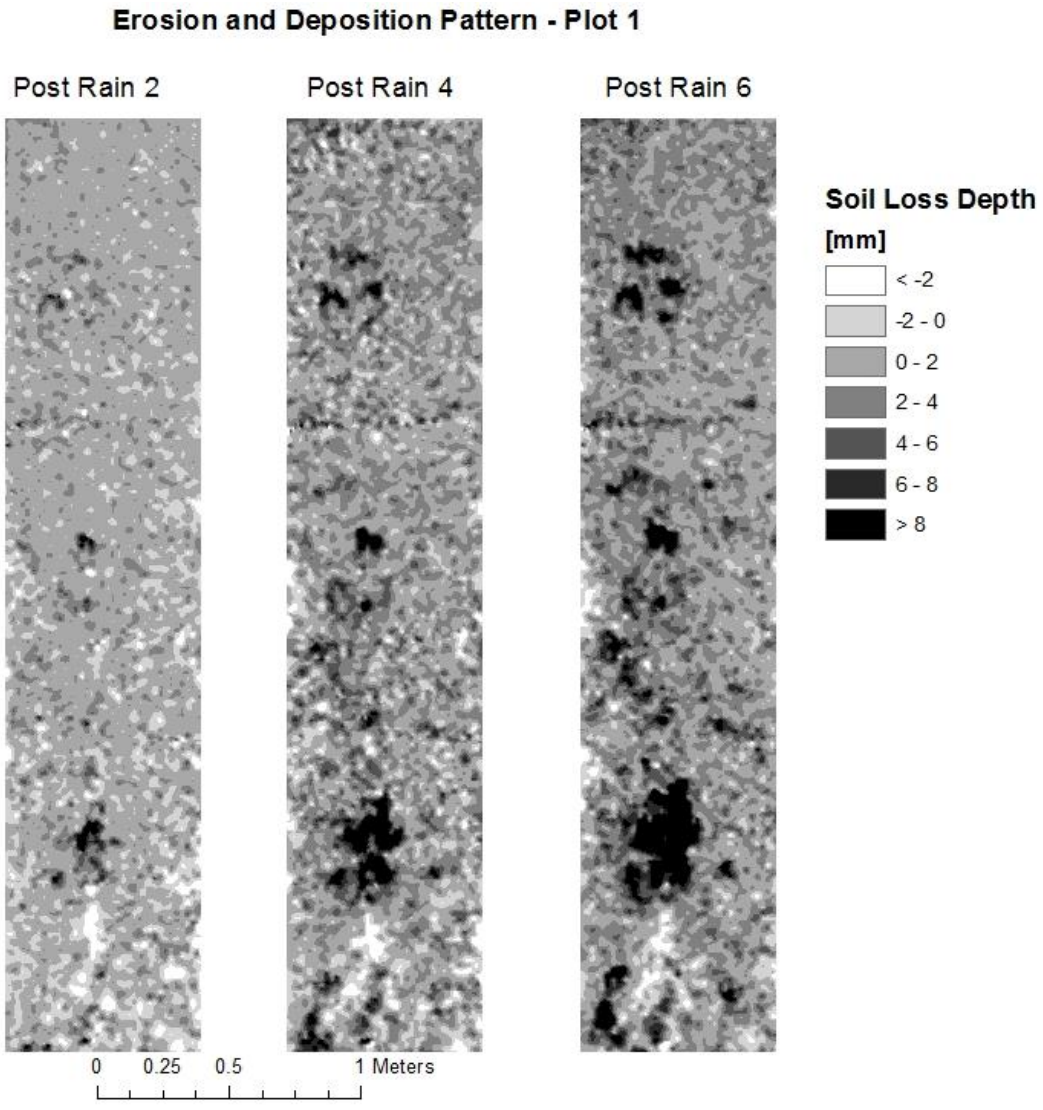

Figure 5.7: Plot 1 progression of erosion and deposition after six rainfall simulations. Soil loss depth is in reference to Rain 1 DEM. Outlet is located at the bottom of the figure.

The erosion and deposition patterns depicted in the plot 1 DEM were consistent with visual inspections. Rills began to form near the outlet after the second rainfall event and get

progressively larger. Several areas of rainfall simulator concentrated drip were observed in the plots. They are represented by an area of excessive erosion and an area of sudden deposition directly downhill. The concentrated drip areas occurred directly beneath the oscillating rainfall simulators trough gaps. At these locations, water would collect on the edges of the diversion pans and drip onto a concentrated plot area (a simulator design flaw). The areas of concentrated drip were aesthetically undesirable, but had no effect on the any of the reviewed methods' ability to measure sediment sources. The methods handled areas of concentered drip in the same fashion as developing rills.

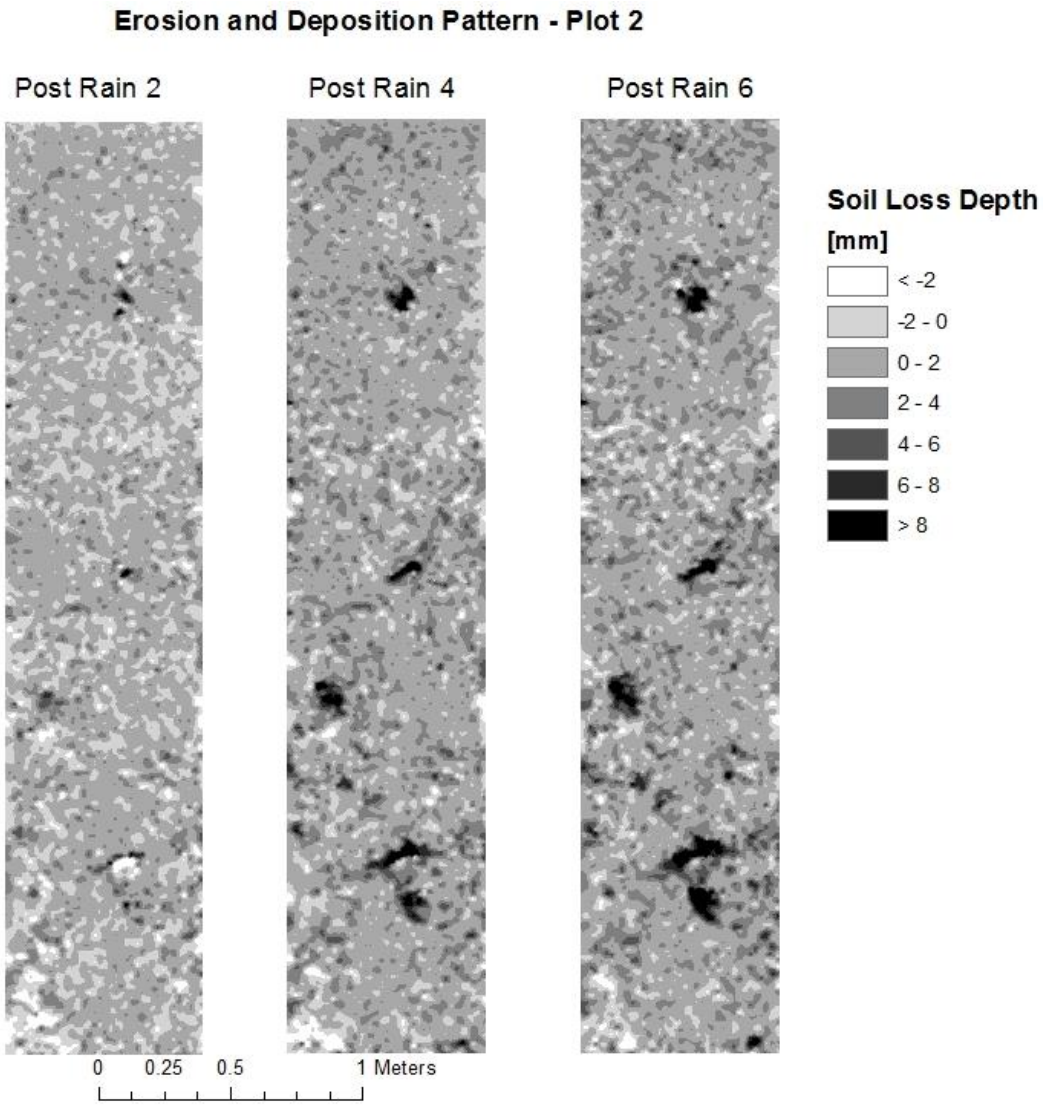

Figure 5.8: Plot 2 progression of erosion and deposition after six rainfall simulations. Soil loss depth is in reference to Rain 1 DEM. Outlet is located at the bottom of the figure.

Differences in soil loss depth were less distinct in plot 2. The areas of concentrated drip were also less apparent than in plot 1. This suggests that there was overall less sediment movement in plot 1.

5.4.2 **Sediment Yields**

Sediment Yields were calculated according to the Ground Based LIDAR methodology. The methodology calculates net volume difference between each simulations DEM. Volume was the translated to grams using the soil's measured bulk density, 1.4 g/cm^3 (Figure 5.9 and Figure 5.10).

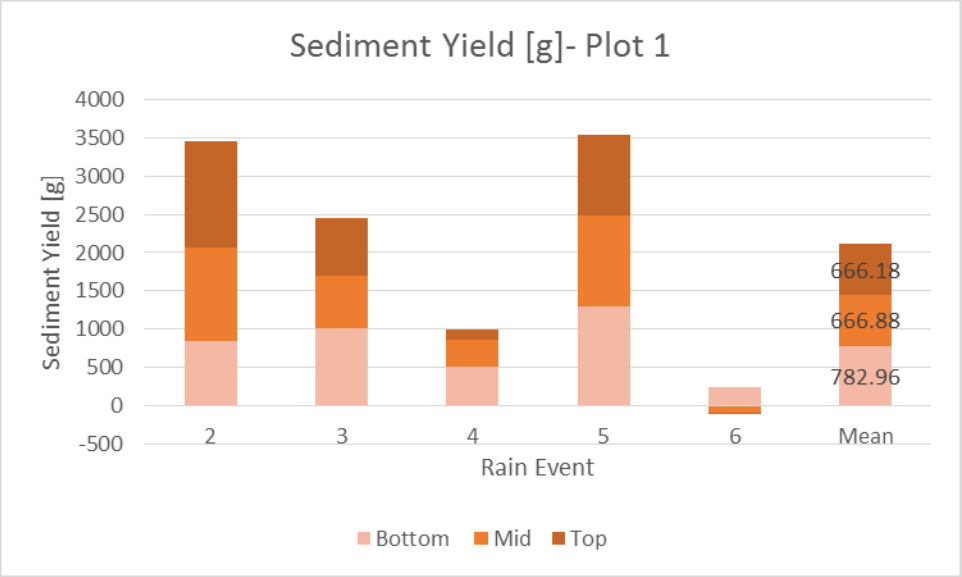

Figure 5.9: Plot 1 section sediment yield [g] per rainfall simulation event

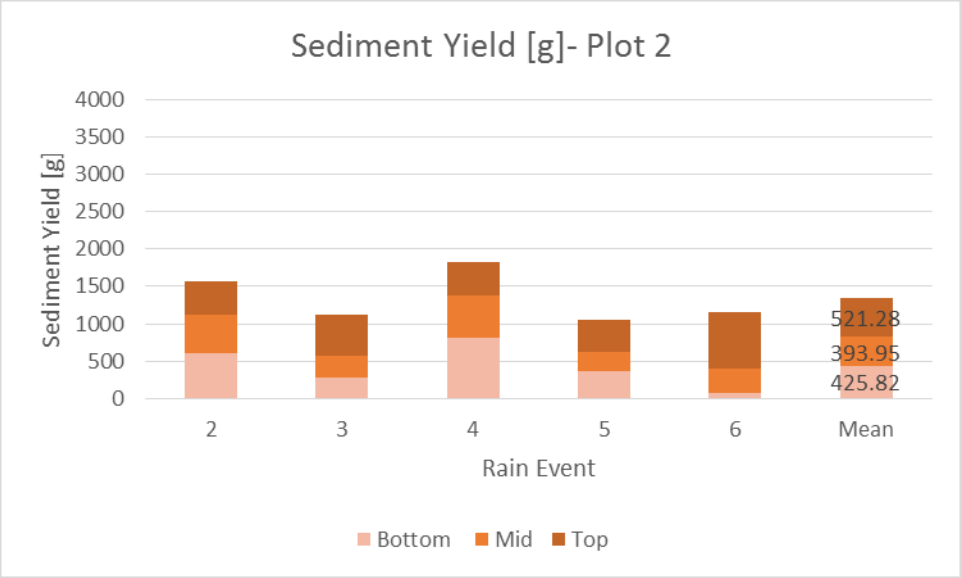

Figure 5.10: Plot 2 section sediment yield [g] per rainfall simulation event

The result shows that from plot 1 31.48%, 31.52%, and 37.52% of the total soil was eroded from the top, middle and bottom sections respectively. From plot 2 38.87%, 29.38%, and 31.75% of the total soil eroded from the top, middle, and bottom sections respectively. This suggests that the main contributing section in plot 1 was the bottom section and from plot 2 was the top section. These results are inconsistent with the analysis from the Interrupted Rill Method. The measured total sediment yields from the LIDAR method are shown to be over predicted when compared to the Interrupted Rill phase 3 runoff sampled sediment yields (Table 5.16).

Table 5.16: Interrupted Rill phase 3 in comparison with LIDAR scan sediment yield. Factor is equal to the ratio of the sediment yields.

	Sediment Yield [g]					
	Plot 1			Plot 2		
Event	Runoff	Scan	Factor	Runoff	Scan	Factor
Rain 2	775.90	3458.73	4.46	566.93	1565.57	2.76
Rain 3	743.20	2450.78	3.30	561.33	1123.63	2.00
Rain 4	629.44	987.98	1.57	611.09	1819.40	2.98
Rain 5	737.06	3543.95	4.81	565.87	1045.02	1.85
Rain 6	596.58	138.64	0.23	556.61	1151.60	2.07
Mean	695.88	2116.02	3.04	491.66	1341.04	2.73

The calculations show that the LIDAR method overestimated the average total plot sediment yield by a factor 3.04 in plot 1 and a factor of 2.73 in plot 2. LIDAR scanned sediment yields between rainfall evets where much less consistent than direct runoff measurements. These overestimation could have many explanations. Some possible causes are operator error and subsidence in the plot soil due to soil settling. These analysis also bring into question the Lecia instrument's capability to measure sediment movement in small amounts. The instrument is

capable of ± 1 mm accuracy. An instrument of this precision may not be applicable in situations where sediment movement is minimal. In situations where sediment movement is more significant, the instrument may perform better. This hypothesis was tested by comparing the cumulative sediment yields of both methods (Table 5.17).

Table 5.17: Interrupted Rill phase 3 in comparison with LIDAR scan cumulative sediment yield. Factor is equal to the ratio of the sediment yields.

Cumulative Sediment Yield [g]

	Plot 1			Plot 2		
Event	Runoff	Scan	Factor	Runoff	Scan	Factor
Rain 2	775.90	3458.73	4.46	566.93	1565.57	2.76
Rain 3	1519.10	5909.51	3.89	1128.26	2689.20	2.38
Rain 4	2148.53	6897.49	3.21	1739.35	4508.60	2.59
Rain 5	2885.59	10441.44	3.62	2305.22	5553.62	2.41
Rain 6	3482.17	10580.08	3.04	2861.83	6705.21	2.34

The sediment yield factor decreases as simulations progress for both plots. This suggests that the Leica 3-D Disto preforms better as a tool for measuring sediment movement as erosion becomes more significant. The hypothesis was further tested with a supplementary experiment utilizing a small sand plot. A determined amount of sand was added to the plot between surfaces scans. As plot the amount of sand added increased, the percent error of the Leica 3-D Disto volume measurements decreased (Table A.1). This supplementary experiment supports the theory that the Leica 3-D Disto may be more applicable for sites with higher sediment movement.

Conclusions

A consistent and repeatable rainfall simulation environment was achieved for the purposes of these experiments. After calibration procedures, the rainfall simulator proved to be a good substitute for natural rainfall. The rainfall simulator's UC was raised for plot 1 and plot 2 from 0.80 and 0.89 to 0.90 and 0.93 respectively. This is much higher than the minimum value of 0.80 recommended in literature. The rainfall intensity for the total plot area was measured to be 55 mm/hr (2.17 in/hr), only slightly greater than the target intensity of 51 mm/hr (2.00 in/hr). It was recorded that plot 1 received slightly higher rainfall depths during the preliminary trials. Because of the high UC and precision of rainfall depths between simulations, this configuration satisfied the objective.

The six REE tracers chosen to for these trials had background concentrations between 1 and 30 ppm, which were comparable to values cited in literature. REE tracers were applied to the soil by two methods, mix and spray, in an attempt to achieve soil tracer concentrations of 10 times their background levels. Soil tracer concentrations were increased with both methods, but the target concentrations were not achieved due to poor soil binding. Eroded sediment from runoff samples showed significant tracer enrichment, which caused the method to overestimate source contributions. However, trends in REE sample concentrations suggested that as simulations progressed, sediment particles originally sourced from the top sections increased in concentration as particles sourced from the bottom section decreased in contribution. This is evidence of top section erosion and deposition on the entire length of the hillslope.

The Interrupted Rill Method was carried out in three phases of simulation. It was assumed that each phase followed the same sedimentation processes. Except for the first simulation event, little variation between sediment concentration and runoff volume was

recorded between simulations within phase. This transferred over to consistent phase sediment yields, where plot 1 experienced slightly hirer rates than plot 2 for each simulation. Instead of tracing specific particles of sediment, as in the REE method, this method strictly measures sediment displacement. It was found that the top section in plot 1 and the middle section of plot 2 had the highest average displacements.

Grounded based LIDAR measurements between rain simulations provided data for the construction of 3-D surface models. The models were first used to analyze erosion depth frequency. The depth of erosion and the range of erosion depths increased as simulations progressed. This was a clear indication of rill development caused by concentrated flow and rainfall simulator concentrated drip. Cut and fill calculations between surfaces were used to calculate sediment yields. It was found that the bottom section in plot 1 and the top section of plot 2 had the highest average displacements. LIDAR sediment yields were shown to overestimate sediment yields in comparison with plot runoff sediment yields. The small volume of erosion that occurred may have been within the instruments range of error. Results show that as erosion volumes become more significant, the performance of the instrument increases.

Measuring sediment by interrupted rills or LIDAR is fundamentally different than using REE tracer concentrating. The LIDAR and interrupted rill method measure net soil displacement, erosion plus deposition, per source section. The REE method traces individual sediment particles down the hillslope and into the runoff bucket. The conceptual difference make the methods difficult to relate to one another. The methods that measure net soil displacement provide more information about what is actually happening on the slope itself. These methods would best answer the question, “Exactly where is erosion and deposition happening”? On the other hand the REE particle labeling method has more to do with exactly

what is happening at the outlet. This method would best answer the question, “From which section is particle sourcing most significant”?

The results from this study showcase each methods inherent strengths and weaknesses. The choice of method relies mostly on its application. Even with the challenges presented in the results, each method was still able to provide much more information than traditional spatially averaged erosion studies. The results of this study indicate that sediment source tracking theory has the potential to increase understanding of soil erosion and deposition processes on a hillslope.

References

Aksoy, H., N. E. Unal, S. Cokgor, A. Gedikli, J. Yoon, K. Koca, S. B. Inci and E. Eris. 2012. A rainfall simulator for laboratory-scale assessment of rainfall-runoff-sediment transport processes over a two-dimensional flume. *Catena* 98(0): 63-72.

ASTM. 2013. Standard Test Methods for Determining Sediment Concentraion in Water Samples. Designation: D3977 - 97 (Reapproved 2013).

Bhattarai Rabin, R., P. K. Kalita, S. Yatsu, H. R. Howard and N. G. Svendsen. 2011. Evaluation of compost blankets for erosion control from disturbed lands. *Journal of environmental management* 92(3): 803-812.

Blasone, G., M. Cavalli, L. Marchi and F. Cazorzi. 2014. Monitoring sediment source areas in a debris-flow catchment using terrestrial laser scanning. *Catena* 123(0): 23-36.

Brooks, A., D. Borombovits, J. Spencer, T. Pietsch and J. Olley. 2014. Measured hillslope erosion rates in the wet-dry tropics of Cape York, northern Australia Part 1: A low cost sediment trap for measuring hillslope erosion in remote areas — Trap design and evaluation. *Catena* 122(0): 42-53.

Cerdà, A., S. Ibáñez and A. Calvo. 1997. Design and operation of a small and portable rainfall simulator for rugged terrain. *Soil Technology* 11(2): 163-170.

Chen, J., H. Xiao, T. Qi, D. Chen, H. Long and S. Liu. 2014. Rare earths exposure and male infertility: the injury mechanism study of rare earths on male mice and human sperm. *Environmental Science and Pollution Research*1-11.

Clarke, M. A. and R. P. D. Walsh. 2007. A portable rainfall simulator for field assessment of splash and slopewash in remote locations. *Earth Surface Processes and Landforms* 32(13): 2052-2069.

Deasy, C. and J. N. Quinton. 2010. Use of rare earth oxides as tracers to identify sediment source areas for agricultural hillslopes. *Solid Earth Discussions* 2(2): 195-212.

Eggert, R. G. 2011. Minerals go critical. *Nature Chemistry* 3(9): 688-691.

EPA, US Environmental Protection Agency. 2012. Rare earth elements: a review of production, processing, recycling, and associated enviornmental issues. EPA 600/R-12/572.

EPA, US Environmental Protection Agency. 2000. Stormwater Phase II Final Rule, Construction Site Runoff Control Minimum Control Measure.

EPA, US Environmental Protection Agency. 1998. National Water Quality Inventory: 1998 Report to Congress, Chapter 3 - Rivers and Streams. 305(b).

Gessesse, G. D., H. Fuchs, R. Mansberger, A. Klik and D. Rieke-Zapp. 2010. Assessment of Erosion, Deposition and Rill Development On Irregular Soil Surfaces Using Close Range Digital Photogrammetry. *Photogrammetric Record* 25(131): 299-318.

Gonzalez, V., D. A. L. Vignati, C. Leyval and L. Giamberini. 2014. Environmental fate and ecotoxicity of lanthanides: Are they a uniform group beyond chemistry? *Environment international* 71(0): 148-157.

HORTON, R. E. 1945. EROSIONAL DEVELOPMENT OF STREAMS AND THEIR DRAINAGE BASINS; HYDROPHYSICAL APPROACH TO QUANTITATIVE MORPHOLOGY. *Geological Society of America Bulletin* 56(3): 275-370.

Huffman, R. L., D. D. Fangmeier, W. J. Elliot, S. R. Workman and G. O. Schwab. 2011. Irrigation Principles. In *Soil and Water Conservation Engineering,* 363. ed. P. McCann, .

Huisman, N. L. H., K. G. Karthikeyan, J. Lamba, A. M. Thompson and G. Peaslee. 2013. Quantification of seasonal sediment and phosphorus transport dynamics in an agricultural watershed using radiometric fingerprinting techniques. *Journal of Soils and Sediments* 13(10): 1724-1734.

Lei, T. W., Q. W. Zhang, J. Zhao and M. A. Nearing. 2006. Tracing sediment dynamics and sources in eroding rills with rare earth elements. *European Journal of Soil Science* 57(3): 287-294.

Lei, T. W., Q. Zhang, J. Zhao and Z. Tang. 2001. A laboratory study of sediment transport capacity in the dynamic process of rill erosion. *Transactions of the American Society of Agricultural Engineers* 44(6): 1537-1542.

Lei, T. W., Q. W. Zhang, J. Zhao, W. S. Xia and Y. H. Pan. 2002. Soil Detachment Rates for Sediment Loaded Flow in Rills. *Transactions of the American Society of Agricultural Engineers* 45(6): 1897-1903.

Liang, T., S. Zhang, L. Wang, H. Kung, Y. Wang, A. Hu and S. Ding. 2005. Environmental biogeochemical behaviors of rare earth elements in soilâ€“plant systems. *Environmental Geochemistry and Health* 27(4): 301-311.

Mao, X. F., Z. Dong and Y. Q. Liu. 2013. Application research on geo-filament bolt reinforced earthen site. *Applied Mechanics and Materials* 353-3541001-1004.

Meijer, A. D., J. L. Heitman, J. G. White and R. E. Austin. 2013. Measuring erosion in long-term tillage plots using ground-based lidar. *Soil and Tillage Research* 126(0): 1-10.

Moazed, H Bavi, A Boroomand Nasab, S Naseri,A Albaji, M. 2010. Effects of climatic and hydraulic parameters on water uniformity coefficient in solid set systems. *Journal of applied sciences* 10(16): 1792-1796.

Moore, I. D., M. C. Hirschi and B. J. Barfield. 1983. Kentucky Rainfall Simulator. *Transactions - American Society of Agricultural Engineers* 26(4): 1085-1089.

Moss, A. J. 1988. Effects of flow velocity variation on rain driven transportation and the role of rain impact in the movement of solids. *Soil Research* 26(3): 443-450.

Narens, L. 2002. A Meaningful Justification for the Representational Theory of Measurement. *Journal of mathematical psychology* 46(6): 746-768.

NRCS. 2007. Natural Resources Conservation Service, 2007 National Resources Inventory - Soil Erosion.

Olmez, I. and F. X. Pink. 1994. New particle-labeling technique for use in biological and physical sediment transport studies. *Environmental science & technology* 28(8): 1487.

Peck, D., P. Kandachar and E. Tempelman. 2015. Critical materials from a product design perspective. *Materials & Design* 65(0): 147-159.

Peter Heng, B. C., J. H. Chandler and A. Armstrong. 2010. Applying close range digital photogrammetry in soil erosion studies. *Photogrammetric Record* 25(131): 240-265.

Polyakov, V. O. and M. A. Nearing. 2004. Rare earth element oxides for tracing sediment movement. *Catena* 55(3): 255-276.

Rickson, R. J. 2006. Controlling sediment at source: An evaluation of erosion control geotextiles. *Earth Surface Processes and Landforms* 31(5): 550-560.

Schertz, D. L. 1983. The basis for soil loss tolerances. *Journal of Soil & Water Conservation* 38(1): 10-14.

Sirvent, J., G. Desir, M. Gutierrez, C. Sancho and G. Benito. 1997. Erosion rates in badland areas recorded by collectors, erosion pins and profilometer techniques (Ebro Basin, NE-Spain). *Geomorphology* 18(2): 61-75.

USDA 2015. Web Soil Survey. Available at: http://websoilsurvey.sc.egov.usda.gov/App/HomePage.htm. Accessed 02/22 2015.

Ventura, E., M. A. Nearing, E. Amore and L. D. Norton. 2002. The study of detachment and deposition on a hillslope using a magnetic tracer. *Catena* 48(3): 149-161.

Vericat, D., M. W. Smith and J. Brasington. 2014. Patterns of topographic change in sub-humid badlands determined by high resolution multi-temporal topographic surveys. *Catena* 120(0): 164-176.

Vinci, A., R. Brigante, F. Todisco, F. Mannocchi and F. Radicioni. 2015. Measuring rill erosion by laser scanning. *Catena* 124(0): 97-108.

Wyttenbach, A., V. Furrer, P. Schleppi and L. Tobler. 1998. Rare earth elements in soil and in soil-grown plants. *Plant and Soil* 199(2): 267-273.

Zhu, M., S. Tan, H. Dang and Q. Zhang. 2011. Rare earth elements tracing the soil erosion processes on slope surface under natural rainfall. *Journal of environmental radioactivity* 102(12): 1078-1084.

Zumdahl, S. S. and S. A. Zumdahl. 2014. *Chemistry, Ninth Edition.* 9th ed. Mary Finch.

Appendix

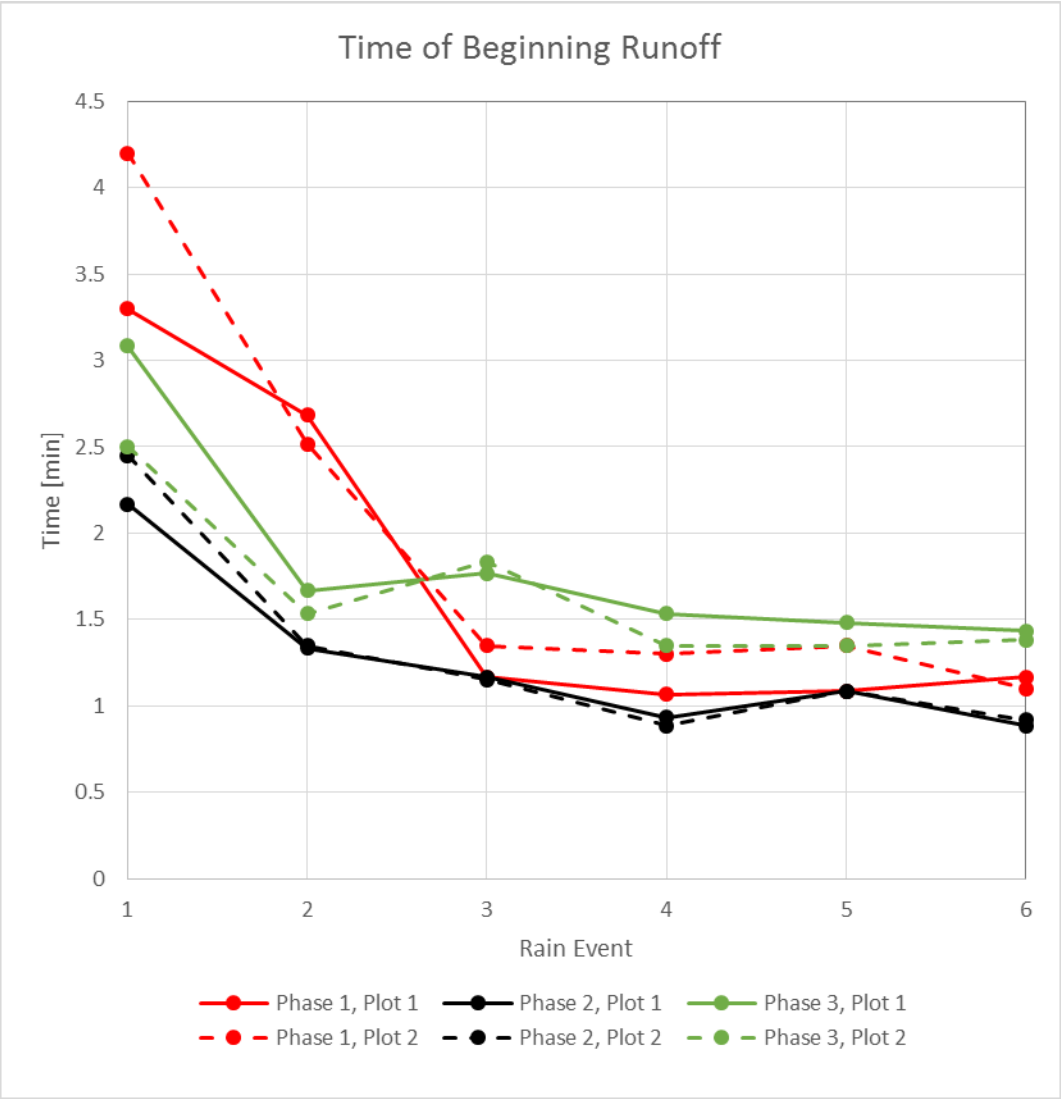

Figure A.1: Time runoff was observed after rainfall simulations began. Higher times suggest greater plot infiltrations.

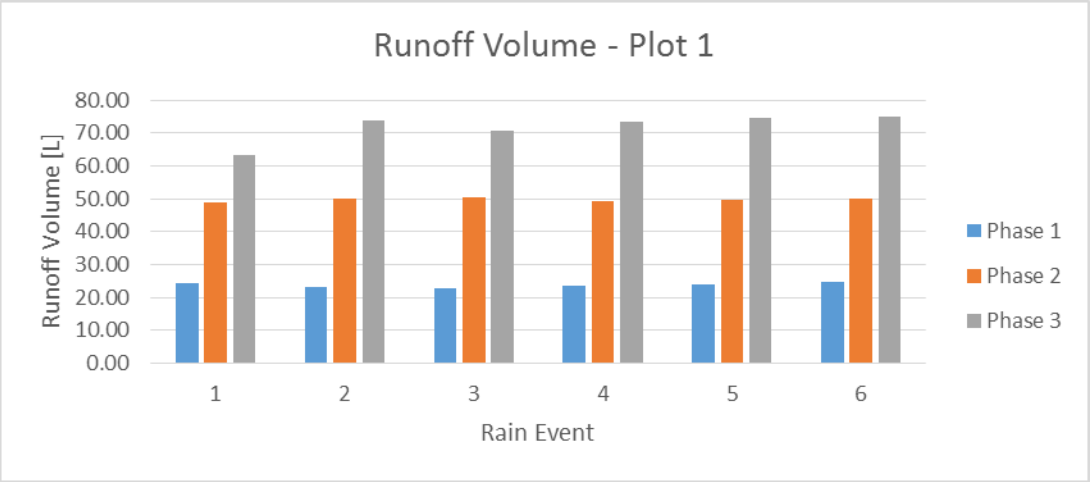

Figure A.2: Recorded phase runoff volumes from plot 1

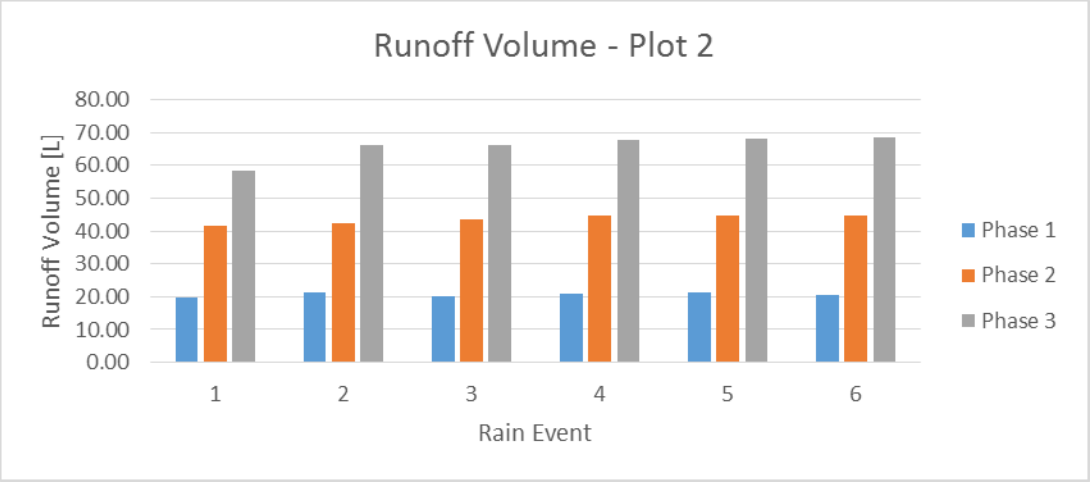

Figure A.3: Recorded phase runoff volumes from plot 2

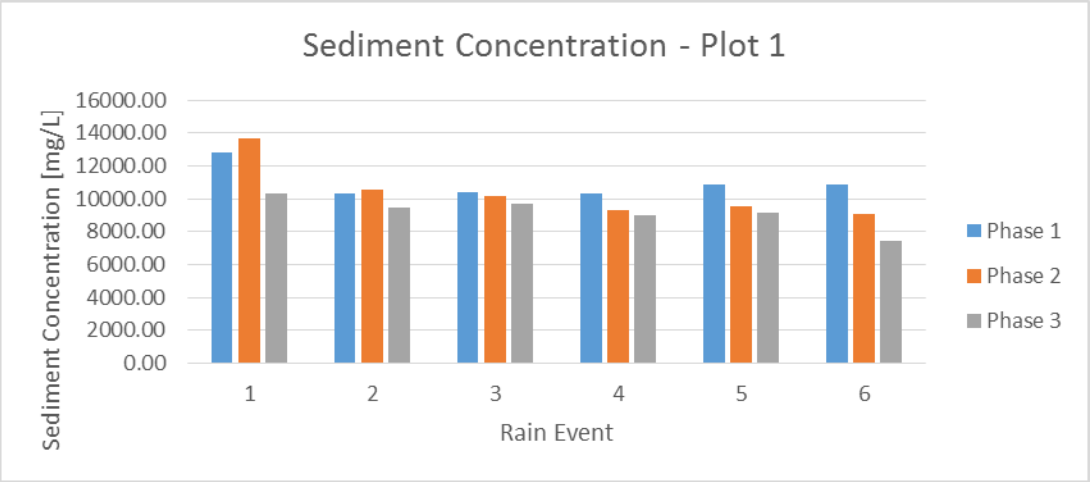

Figure A.4: Determined phase sediment yields form plot 1

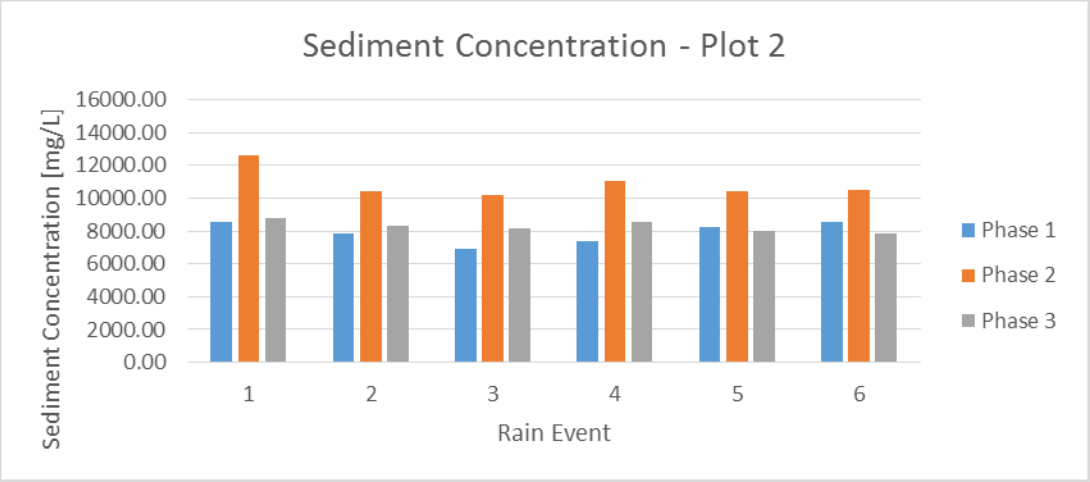

Figure A.5: Determined phase sediment yields from plot 2

A supplementary experiment was undergone to test the capability of the Lecia 3D Disto as a surveying tool to create 3D soil surface models for soil cut and fill analysis.

A method was developed to evaluate the Leica 3D Disto's performance at making soil surface measurements on a small plot. A small soil plot was constructed in the lab for this analysis. The plot border was constructed of standard 1.9 x 3.8 cm pine lumber. Four pieces of wood were cut to a length of 76.9 cm and screwed together to create a rectangular frame. The rectangular frame had inside dimensions of 75 x 75 cm. The frame was then placed flat on a concrete floor forming a boxed area to contain the soil media. Fine sand was the chosen soil media for the experiment. Sand was the ideal material for this experiment because it is resistant to clumping and lacks structure which is found in many other soils. The plot was filled to the brim with sand and leveled with a wooden screed. After the sand was in place, four PVC targets were place in the sand at the plot corners. The targets would be stationary and used as reference points for the laser to locate during surface scans.

The Lecia 3D Disto was then used to scan the surface of the sand plot. The first scan was to be used as the reference surface from which cut and fill volumes of subsequent scans would be computed. After the reference surface was taken, known volumes of sand were added to the plot surface. The Lecia 3D Disto was then tasked with measuring the surface after each volume addition. Sand was added to the plot five times with volumes ranging from 250 to 5000 cc. This approach tested the Lecia 3D Disto's capabilities at measuring volume changes on small and large scales. The results are presented in Table A.1.

Table A.1: Sand scan volume and measured volumes comparisons

Sand Scans

Volume	Scan 1	Scan 2	Scan 3	Scan 4	Scan 5
Sand Added [cc]	250	500	1000	2000	5000
Measured [cc]	318.4	691.3	1056.9	2052	5187.5
Factor	1.2736	1.3826	1.0569	1.026	1.0375